91-03635/

ANALYSIS OF GOSSANS AND EXPLORATION GUIDES, HAWK HILL-GRIFFIN-MOUNTAIN LAKES AREA DISTRICT OF KEEWATIN

Lawrence B. Aspler
March 1990

NWT GEOLOGY DIVISION - NAP
Box 1500 - Yellowknife

Indian and Northern Affairs Canada
Affaires indiennes et du Nord Canada

EGS 1990-7 Analysis of Gossans and Exploration Guides, Hawk Hill-Griffin-Mountain Lakes Area, District of Keewatin part of NTS 65 C Canada - NWT Mineral Development Agreement; by L.B. Aspler 1 text, 65 p.

Price: $3.80.

CANADA N.W.T.
MINERAL DEVELOPMENT AGREEMENT

ANALYSIS OF GOSSANS AND EXPLORATION GUIDES,

HAWK HILL-GRIFFIN-MOUNTAIN

LAKES AREA, DISTRICT OF KEEWATIN

LAWRENCE B. ASPLER

MARCH, 1990

INDIAN AFFAIRS AND NORTHERN DEVELOPMENT (YELLOWKNIFE)

OPEN FILE EGS 1990-XX

Contribution to the Canada-Northwest Territories Mineral Development Agreement 1987-1991, carried jointly by Geological Survey of Canada, Indian and Northern Affairs Canada (Yellowknife) and Government of the Northwest Territories.

CONTENTS

ABSTRACT 3

INTRODUCTION 5

STRATIGRAPHIC, SEDIMENTOLOGIC AND STRUCTURAL SETTING 6

ANALSIS OF GOSSANS 8

GOSSANS IN BASEMENT 8

GOSSANS IN THE HURWITZ GROUP 9

PADLEI FORMATION 9

KINGA FORMATION 9

AMETO FORMATION 11

WATTERSON FORMATION 12

TAVANI FORMATION 13

DISCUSSION: GUIDES FOR EXPLORATION 14

ARCHEAN-HOSTED GOLD 15

DEEP-LEVEL DETACHMENT SURFACES 15

SHALLOW-LEVEL DETACHMENT SURFACES 17

CROSS FAULTS THAT TRANSECT THE BASEMENT-COVER CONTACT 18

SHEAR ZONES PARALLEL TO THE BASEMENT-COVER CONTACT 18

PROTEROZOIC-HOSTED GOLD 19

ACKNOWLEDGMENTS 20

FIGURE CAPTIONS 21

TABLE CAPTIONS 22

REFERENCES CITED 23

FIGURES 26

TABLES 38

ABSTRACT

The Hurwitz Group represents aborted rift (Padlei Formation glacigenic ? conglomerate and fluvial conglomerate, arkose and siltstone) and cratonic basin (Kinga Formation granulestone and quartz arenite) sedimentation that was interrupted by emergence (Hawk Hill Member silcrete) and drowning (Ameto Formation slate and arkose). Shoaling-upward sequences in the Ameto, Watterson, Ducker and Tavani formations, with short-distance lateral facies changes, indicate repeated development of short-wavelength bulges and depressions. The bulges and depressions are either collision-related, thrust load-induced (forebulge/foredeep model) or non-collision related, intraplate stress-induced (arch/depression model).

Shallow-level Proterozoic shortening was by thick-skinned basement-cover infolding; thrusting is limited to minor out-of-syncline structures. NW-trending, upright, concentric D1 folds are refolded by E and NE-trending upright (and locally inclined), concentric, D2 folds, generating dome and basin (and locally mushroom) interference patterns. Interference is inferred to be a consequence of superposed folding, with active north-south shortening overprinting northwest structures. It is uncertain if the interference represents episodic versus polyphase deformation. Folding was primarily by flexural slip accompanied by tangential longitudinal strain; minor thrusts, cross faults, joints, disharmonic folds, and fold and cleavage fans are space-accommodating. Changes in basement rock type and structural grain provided anisotropies that influenced Hurwitz thickness and facies and guided Proterozoic deformation. Basement anticlinoria, with a wavelength of about 35 km, separate the Hawk Hill area from synclinoria east at Ducker Lake and west at Watterson Lake. Regional shortening at shallow crustal levels by basement-cover infolding may be balanced at depth by regional intrabasement detachment. The link between the Hawk Hill (and Watterson) areas and the Poorfish-Windy Thrust/Fold Belt may be a

detachment that cut to surface to emplace hot basement over cold cover immediately east of the Poorfish-Windy Belt.

Structural analysis suggests that both the "Shear lake" and "B-Zone" deposits (past gold-producers near Cullaton Lake) formed as a consequence of Proterozoic strain. Systematic measurement of fractures in Kinga Formation quartz arenites documents trends that are not regionally consistent but reflect heterogeneous strain of both D1 and D2 folds: fractures and cross faults formed due to outer arc extension and inner arc shortening during tangential longitudinal strain . The fractures are sites of pyrite-gold, similar to the Shear lake deposit where joint patterns indicate hinge-zone extension in the outer arc of a D2 fold (A.R. Miller, unpub. data). A genetic relationship between folding, cross faulting, jointing and Shear lake-type mineralization is suggested.

At the Cullaton B Zone, analysis of subsurface data suggests that zones of chloritic alteration, quartz stockworking and gold mineralization in Archean iron formation is spatially restricted to shallowly dipping faults and fold axial surfaces (A.R. Miller, p. comm. 1989) that are probably Proterozoic structures. Similarly, gold values in Archean rocks at Lothrop Lake (A.R. Miller, unpub. data) and Hawk Hill Lake are in the hinge zones of Proterozoic folds. Geometric constraints of concentric folding imply intrabasement detachment both as local space accommodating structures (in fold cores) and as regional-scale structures that balance shortening at depth: either may have served to localize Proterozoic gold in Archean rocks.

In the past, the primary exploration targets in the area have been the Archean supracrustal sequence (especially BIF) and Proterozoic Kinga Formation quartz arenites. Prospecting during the course of mapping has opened new exploration targets. The discovery of structurally-controlled gold in stratigraphy above the Kinga Formation suggests that any unit in the sequence may host gold-rich shear zones, fractures and quartz veins. Indeed, the highest value determined from the present

mapping (0.966 oz./ton, 33,100 ppb Au) is from a quartz-pyrite veined sheared calcareous arkose of the Watterson Formation. In addition, although gold values from cm-dm-scale pre-compaction massive pyrite concretions at the top of the Ameto Formation are typically below background (<1 ppb) local elevated values open the possibility of early diagenetic, stratigraphically-controlled mineralization. First order exploration targets include: 1) fold hinge zones, cross-faults and thrusts in any unit of the Hurwitz and Kiyuk groups; and 2) Proterozoic detachment surfaces and folds within Archean rocks.

INTRODUCTION

The Hurwitz Group is presently exposed as a discontinuous chain of outliers that extends from Hudson Bay to Ennadai Lake (Fig. 1). The outliers represent the erosional remnants of synclinoria infolded with basement and relics of thrust-fold belts. Some may reflect an original sub-basin geometry. Most of the Hurwitz belt has been mapped at a reconnaissance level only. Hence the goals of the present study were to undertake: 1) fundamental basin analysis (determining depositional systems, stratigraphic and facies relationships, in order to establish basin configuration, subsidence mechanisms and tectonic significance); 2) structural analysis (to determine the relative importance of thrusting versus basement-cover infolding and resolve the significance of a vergence pattern that is regionally inconsistent); and 3) mineral resource assessment; to actively prospect during the course of mapping and (by understanding the basic geological framework) to establish a context for known deposits and to define future exploration targets.

Two areas were mapped at a 1:50,000-scale: the Poorfish Windy belt in 1988 (Aspler, 1988, 1989a; Aspler *et al.*, 1989); and the Hawk Hill-Griffin-Mountain lakes area in1989. Below are presented field petrographic and geochemical data from gossans found in the Hawk Hill-Griffin-Mountain lakes area that compliment previous

releases (Aspler, 1989 b; Aspler and Bursey, 1990; Bursey and Aspler, 1990). Coupled with stratigraphic and structural analysis, these data are used to specify a geological rationale for the previously-mined "Shear lake" and "E zone" gold deposits at Cullaton Lake, and to establish predictive models for future exploration.

STRATIGRAPHIC, SEDIMENTOLOGIC AND STRUCTURAL SETTING

Essential elements of the stratigraphy and sedimentology of the Hawk Hill-Griffin-Mountain lakes area are summarized in Figure 1 B and in Table I. Previously (Aspler, 1989; Aspler *et al.*, 1989) the post-Kinga Formation Hurwitz Group stratigraphy was interpreted in terms of a foredeep model, with cycles of sedimentation being related to ca. 1.81-1.87 Ga collision in Trans-Hudson Orogen (Fig. 2). However, preliminary U-Pb baddeleyite geochronolgy on Hurwitz gabbros (L. Heaman, p. comm. 1989) and stratigraphic arguments (see Aspler and Bursey, 1990 for details) indicate that the Hurwitz Group may be ca. 2.1 Ga, ie. older than any known collisional event in Trans-Hudson Orogen . Hence, if evidence for an older cryptic collision, presently masked by younger events, is not found, the only true foredeep deposits may be the Hurwitz "H" and Kiyuk Group units of Aspler *et al.* (1989). An alternative model that may account for the vertical, and short-wavelength lateral, facies changes in Hurwitz Group stratigraphy considers the role of intraplate stress (Fig. 3). When superposed on an existing subsidence process, such as thermal subsidence in a cratonic basin, ridge-push generated intraplate stresses are of sufficient magnitude to cause crustal deflections which may simulate foredeep-forebulge interaction (Cloetingh, 1988). As a working model, the Hurwitz Group may represent sedimentation in a cratonic basin coeval with development of the Wollaston Group passive margin (see Lewry *et al.*, 1985). The intraplate stresses may have been generated along a ridge in the

Manikewan Ocean (Stauffer, 1984) that ultimately closed, with subduction of Manikewan oceanic crust resulting in formation of the Wathaman Batholith.

In contrast to the Poorfish-Windy Thrust-Fold Belt, the structural style in the Hawk Hill-Griffin-Mountain lakes area is one of basement-cover infolding, with thrusts being limited to minor out-of-syncline space accommodating structures (Figs. 4, 5). The fundamental structure of the area is that of a broad synclinorium of Hurwitz Group rocks in basement. Northwest-trending, concentric, upright D1 folds are refolded by east and northeast-trending, concentric, upright (and locally inclined) D2 cross folds, generating dome and basin Ramsay Type I (and locally mushroom-like Type I-II) interference patterns (see Ramsay and Huber, 1987). Interference is inferred to be a consequence of superposed folding, with active north-south shortening overprinting northwest structures, but it is unknown if the folding represents episodic versus progressive polyphase deformation. The east-west structures are considered to be "D2" because they locally refold northwest-trending D1 axial surfaces and D1 limbs, and D2 cleavage is not deflected about D1 trends.

Both fold sets represent thick-skinned crustal shortening whereby basement and cover are folded together. Flexural slip, including cover over basement, and tangential longitudinal strain are regarded as having been the primary folding mechanisms. Minor map-scale thrusts, variably oriented oblique-slip cross faults, joints, disharmonic folds and fold and cleavage fans are regarded as space accommodating structures (upper detachment in concentric folding, see Dahlstrom, 1970). Basement rock type and structural grain may have influenced Proterozoic deformation both by exerting a control on stratigraphic thickness of the cover and by providing anisotropies that guided deformation (see Aspler and Bursey, 1990 for details).

Basement anticlinoria, with a wavelength of about 35 km, separate the area from synclinoria east at Ducker Lake and west at Watterson Lake. The link between

the present area (and the Watterson area) and the Poorfish-Windy Belt may be a regional-scale intrabasement detachment (Fig. 6). As will be discussed below, definition of the structural style and the geometric consequences of the style at depth, have important economic implications.

ANALYSIS OF GOSSANS

Table II summarizes field and petrographic descriptions and analytical work on 54 samples from 44 gossans. Gossan locations are specified on Figure 7 and by UTM coordinate in Table II. Except where noted, all chemical analyses were performed by X-Ray Assay Laboratories, Don Mills Ontario. Analytical methods and detection limits are indicated in Table II. The discussion below highlights gossans with anomalous values, (particularly gold, see summary in Table III) and considers mineral paragenesis.

GOSSANS IN BASEMENT

The highest Archean-hosted gold value is from a quartz vein that cuts granitic rocks close to an intrusive contact with mafic volcanic rocks: 130 ppb Au with 1300 ppm Cu and 100 ppm Pb (sample 87-11, locality 16). Clusters of pyrite and chalcopyrite are disseminated in the quartz vein. As will be discussed below, the quartz vein is in the hinge zone of a Proterozoic fold (Fig. 1) and is considered to have formed during Proterozoic strain.

Sample 101-13 (locality 10, southwest of Griffin Lake) yielded 15 ppb Au, 130 ppm Co and 71 ppm Zn. The sample is of a well-layered mafic tuff with up to 20% pyrite distributed along the layering. The tuff is part of the Archean volcanic sequence. It is interlayered with massive mafic volcanic rocks and is cut by well-foliated gabbroic and granitic bodies. Southwest of Griffin Lake, the unit is preserved as discontinuous

lenses between younger granitic rocks on the west and the structural contact with the Hurwitz Group on the east.

No other samples from the Archean sequence yielded high gold values although two from the arkose-slate turbidite sequence east of Mountain Lake (63-9A and 63-9B, locality 30) were slightly anomalous in silver (1.0 ppm and 0.5 ppm respectively).

GOSSANS IN THE HURWITZ GROUP

PADLEI FORMATION

Only one sample from the Padlei Formation, a granule-pebble mixtite, yielded a value above the typical <1ppb: 2 ppb Au (sample 66-10B, locality 33). Although the gold value is trivial, the sample contains 2 ppm Ag, the highest recorded. It is uncertain if the gold value represents a paleoplacer versus structure-controlled concentration.

KINGA FORMATION

Twelve samples of Kinga Formation quartz arenite were above background in gold. Values are low on samples from gossans consisting of irregular hematitic stains along joint surfaces (sample 73-6, locality 35: **7 ppb Au**; sample 71-5A, locality 37: **3 ppb Au;** sample 67-11, locality 40: **3 ppb Au;** sample 78-11C, locality 42: **2 ppb Au**). Greater values were recorded from samples with visible pyrite (+/- chalcopyrite) (sample 97-11, locality 4: **23 ppb Au**; sample 96-2, locality 5: **230 ppb Au**; sample 97-2, locality 7:**13 ppb Au**, sample 102-7, locality 8: **57 ppb Au**; sample 101-33, locality 12: **23 ppb Au;** sample 94-8A, locality 23 **56 ppb Au**; sample 94-8B, locality 23: **80 ppb Au,** also with **293 ppm U**). The highest value was from an outcrop of intensely jointed quartz arenite in which quartz arenite breccia fragments are cemented by specular hematite and chlorite (**460 ppb Au**, sample 73-7B, locality 36).

Lord (1953, p. 9) reported 0.01 oz/ton Au and 0.09 oz/ton Ag from a sample of quartz arenite southwest of Griffin Lake.

Structural control on gold distribution in all examples is demonstrated by restriction of anomalous values to joint and/or shear surfaces (eg. Fig. 8A); sulphide/oxide minerals dissipate away from these structures to barren quartz arenite. Examples of quartz arenite mosaic breccia (see Laznicka, 1989) cemented by chlorite and sulphides (Fig. 8B) or specular hematite (Fig. 8C) suggest a process of progressive fracturing and annealing, with joint development concurrent with fluid introduction, chloritization and, depending on local spatial or temporal variation in oxygen and sulphur fugacity, sulphide or oxide growth. Strain probably outlasted pyrite growth (see Fig. 8D).

Joints were measured continuously during mapping using the selection method of Goldstein and Marshak (1988), in order to test if they formed during, and as a consequence of, regional folding rather than having formed in a later unrelated stress field. Joint orientations are not consistent regionally, but reflect heterogeneous strain of both D1 and D2 structures (Fig. 9). Where D2 folds are predominant, joint sets (and cross faults) are consistent with outer arc extension and inner arc shortening under tangential longitudinal strain (see Ramsay and Huber, 1987, Fig. 21.18). Similarly, fracture patterns indicate shortening across well-developed D1 structures. Where both D1 and D2 structures are prominent, fracture patterns are complex and sets related to both are developed (Fig. 9). Hence a genetic relationship between regional D1 and D2 folding, cross faulting, jointing and mineralization is indicated. The style is similar to that of the Shear Lake deposit southwest of Cullaton Lake (Raman *et al.*, 1986, Miller, 1989) in which quartz arenite-hosted epithermal mineralization is within fractures and cross faults formed by hinge zone extension in the outer arc of a D2 fold (A.R. Miller, unpub. data). This style is not restricted stratigraphically to the Kinga Formation; gold in units higher in the section may have a similar origin (see below).

An additional structure-specific site of mineralization is indicated by a sample at the sheared basement-cover contact in which massive and disseminated pyrite and local chalcopyrite are distributed along , as well as across, contact-parallel mylonitic layering (23 ppb Au, sample 101-33, locality 12).

One sample at the base of the type section of the Hawk Hill Member (Aspler and Bursey, 1990) was slightly above background in gold : 3 ppb Au (S-4-C, locality 26). The vertical profile consists: of pristine quartz arenite; a transition zone (0.5 m thick) marked by the appearance of clay alteration in fractures and around detrital quartz grains and maroon oxidation spots in the quartz arenite; a 0.5 m thick layer of white laminar silcrete; and breccia of white chert fragments in maroon chert/specular hematite cement. The low gold value is from the white laminar chert unit, none of the samples of silcrete breccia (S-10, S-11, 88-4B) were greater than <1 ppb Au. The gold may have formed from lateral transfer into the lower part of the paleoweathering profile under oxidizing conditions (see eg. Clemmey, 1985; Lawrance, 1988).

AMETO FORMATION

The most visually impressive gossans are from weathering of massive pyrite concretions in the Ameto Formation, south-central Hawk Hill Lake (Fig. 10, localities 19, 20, 21, 22). The concretions are stratigraphically confined to the top of the unit as it undergoes a vertical facies transition, shallowing upward to the Watterson Formation. The shallowing -upward is manifested by an increase in the number and thickness of cross-stratified arkose layers (at the expense of slate) in Bouma-like cycles, appearance of wave ripple cross-stratified arkose (from storm? wave reworking of sandy layers) and appearance of local cryptalgal laminate layers (Table I).

The concretions are typically within the arkose interlayers, they range from <1 to 20 cm, have ovoid shapes, are distributed along bedding planes and are either discrete or linked laterally by bedding-parallel protuberances. Bedding wraps around

the concretions, indicating a pre-compaction origin. Smaller concretions tend to be elongate along pressure solution cleavage, due to dissolution of original boundaries. Larger concretions, and those laterally linked, maintain a bedding-parallel elongation. A pre-strain origin is confirmed by observation in thin section of quartz-chlorite pressure fringes in pressure shadows (Fig. 10 B). In addition to the large concretions, mm-scale pyrite is disseminated within arkose and slate beds, distributed either randomly or along bedding. These disseminations engulf detrital quartz grains (Fig. 10 C) but are elongate along pressure solution cleavage, again suggesting a pre-strain, diagenetic origin.

Despite being visually impressive, the concretions did not yield high gold or base metal values. Two samples were above background in gold (80-3A, **4 ppb Au**; 80-5E, **2 ppb Au)**, one was above background in lead (80-12, **320 ppm Pb**) and all were relatively high in manganese (greater than 500 ppm, maximum of 1200 ppm, sample 80-5D).

A sample of slate with intense hematitic alteration along bedding, cleavage and fractures from lower in the section (67-2B, locality 38) gave a result of 3 ppb Au and was above background in silver (1ppm), copper (67 ppm) and zinc (50 ppm). A similar sample (72-7, locality 39) was above background in silver (2 ppm) and zinc (58 ppm).

WATTERSON FORMATION

The highest gold value determined from the present study is from a quartz-pyrite vein stockwork within highly strained calcareous arkose of the Watterson Formation. The stockwork is related to movement along an oblique-slip D2 cross fault (sample 100-11A, locality 1). The showing is on the west-facing scarp of an island in the river linking Griffin and Mountain Lakes (Fig. 7). The island was visited on foot from the

southern mainland in mid-August 1989; it is unknown to what extent spring flooding may prohibit access earlier in the year.

The preliminary value of > 10,000 ppb Au (gold concentration too high for measurement by FADCP method) reported previously (Aspler and Bursey, 1990) has been confirmed by a fire assay on a fraction of the pulp used for the initial analysis performed by Terramin Research Laboratories Calgary for Suncor Inc., Calgary: 0.966 oz/ton or 33,100 ppb Au (S. Safton, p. comm. 1990). A second fire assay on a portion of the original hand specimen yielded 0.233 oz/ton (7980 ppb; S. Safton, p. comm. 1990). Accompanying the high gold content are elevated cobalt (160 ppm) and nickel (260 ppm).

The gold occupies three textural sites: 1) filling microfractures in pyrite up to 20 μm wide and 200 μm long (Fig. 11 A); 2) as 0.1-5.0 μm inclusions within pyrite; and 3) as 10 μm disseminations (with iron oxides) in host rock fractures.

A sample of Watterson Formation calcareous siltstone from the lateral continuation of the same outcrop (sample 100-11B, locality 2) was also anomalous in gold (64 ppb Au), cobalt (150 ppm) and nickel(130 ppm). In contrast to locality 1, the pyrite is not part of a stockwork, but forms random disseminations up to 2mm (with local chalcopyrite and hematite inclusions) and is considered to be pre-strain (diagenetic ?) as indicated by calcite-quartz pressure fringes (Fig. 11 B). Hence structurally-controlled enrichment of early (diagenetic ?) gold is possible.

TAVANI FORMATION

Three samples of Tavani Formation sub-arkose (with cryptalgal laminate lenses) were above the detection limit (<0.5 ppm) in silver (samples 97-5A, 1.0 ppm Ag; 97-5B, 0.5 ppm Ag, locality 9; sample 70-7, 1.5 ppm Ag, locality 43). One of these (sample 97-5B) had above background gold (6 ppb Au). Both localities are adjacent

D2 faults, pyrite, hematite and calcite form fracture fills and/or disseminations in stockwork breccias.

DISCUSSION: GUIDES FOR EXPLORATION

Past exploration in the Hawk Hill-Griffin-Mountain Lakes area in the 1940's by Hudson Bay Mining and Smelting, the 1960's by Selco Exploration Canada Ltd., and the 1980's by Suncor Inc. and Cullaton Lake Gold Mines Ltd. (Eade, 1974; Raman et al., 1986) concentrated on the search for Archean lode gold, and gold in fractured Hurwitz Group quartz arenite. Between 1981 and 1985, gold was mined from the "B-Zone" (Archean BIF-hosted) and "Shear Lake" (Hurwitz Group quartz arenite-hosted) deposits southwest of Cullaton Lake by Cullaton Lake Gold Mines Ltd. (Raman *et al.*, 1986; Miller, 1989).

Important implications for future exploration suggested by this study include: 1) definition of a new genetic model for Archean-hosted B-Zone type gold; and 2) definition of a geological rationale for Shear Lake type gold, and extension of the Shear Lake model to units higher in the Hurwitz Group. These will be discussed in turn below. Worthy of emphasis is the observation that the highest gold value from the present study is neither from the Archean package, nor from Kinga Formation quartz arenites, but from deformed rocks of the Watterson Formation. This result is consistent with data from the Poorfish-Windy belt in which anomalous gold values were found above the Kinga Formation, in Hurwitz Group and Kiyuk Group stratigraphy (Ameto Formation, maximum of 100 ppb; Watterson Formation, maximum of 150 ppb; Tavani Formation, 110 ppb; Kiyuk Group, maximum of 1660 ppb; Aspler, 1989a). These data confirm the conclusion in Aspler (1989a) that the Proterozoic supracrustal package is a viable, and as yet largely untested, target for economic deposits.

ARCHEAN-HOSTED GOLD

Archean-hosted gold showings in the area have previously been regarded as syngenetic, volcanogenic exhalite deposits (particularly those associated with banded iron formation, eg. Page, 1979), or as modified syngenetic deposits in which gold, remobilized and enhanced by Archean metamorphism and deformation, was concentrated in Archean structures (Eade, 1974; Raman *et al.;* 1986; Miller, 1989). Analysis of structural data from the present study and evaluation of the structural setting of Archean-hosted gold at the Cullaton B-Zone, at the "Lothrop lake" prospect, at the Cullaton Shear Lake deposit, and southwest of Hawk Hill, suggests a third model. This model differs from those previously considered in two respects: 1) gold is envisioned to have formed as a consequence of Proterozoic strain and concentrated in Proterozoic structures developed within Archean rocks, and 2) gold concentrated by Proterozoic structural processes is not necessarily restricted to a particular (eg. BIF) host.

Four principal Proterozoic structures are developed in Archean rocks of the area: 1) deep-level detachment surfaces; 2) shallow-level detachment surfaces; 3) cross faults that transect the basement-cover contact; and 4) shear zones along the basement-cover contact. All are genetically related to regional shortening either by basement-cover infolding (at shallow structural levels) or regional thrusting (at deep structural levels). The analysis below suggests that all four are potential gold targets.

DEEP-LEVEL DETACHMENT SURFACES

As outlined above, the Proterozoic structural style in the map area is one of large scale basement-cover infolding (eg. Figs. 1,4,5). Shortening by basement-cover infolding at shallow structural levels is required to be balanced at depth within basement, by distributed strain or detachment (see Fig. 31 in Dahlstrom, 1970; Stewart, 1987; Hoffman *et al.*, 1988). As illustrated in Figure 6, the geometric link

between the present map area (and the Watterson area) to the Poorfish-Windy Thrust-Fold Belt may be such a regional scale intrabasement detachment. The detachment is regarded as having emplaced hot basement over cold cover, accounting for the eastward increase in metamorphic grade of Hurwitz Group rocks in the Poorfish-Windy belt. The fault that juxtaposes basement over actinolite-bearing, Tavani Formation rocks (highest metamorphic grade in the map area) east of the Kognak River in the northeast portion of the map area (Fig. 1) may be where a detachment rooting to the east beneath the basement anticlinoria that separates the map area from Hurwitz rocks at Cullaton Lake, breached to surface.

Gold in the Cullaton B-zone and "260-zone" (Raman *et al.*, 1986) may be related to similar intrabasement detachments. From analysis of subsurface data at the Cullaton mine site, Raman *et al.*, (1986) and Miller (unpub. data) described shallowly-dipping faults and folds with shallowly-dipping axial surfaces and shallowly-plunging hinge-lines. Archean folds in the area have a different geometry, with near-vertical axial surfaces and near-vertical (locally downward-facing) hinge lines (Fig. 1; Miller, unpub. data). The shallowly -dipping structures referred to above cut near-vertical iron formation. Hence the configuration is one of pre-existing Archean structures with steep attitudes being cut by later structures with shallow attitudes (see also Fig. 7 in Raman *et al.*, 1986). It is suggested here that the structures with shallow attitudes are related to Proterozoic shortening at depth, and that faults such as the "260 fault" (Raman *et al.*, 1986) are Proterozoic intrabasement detachments. Critical to the argument of Proterozoic gold in Archean rocks is the spatial association to what are considered Proterozoic structures. That is, zones of chloritic alteration, quartz stockworking and gold mineralization are not spatially associated with Archean structures, but are restricted to shallowly dipping Proterozoic hinge lines and faults (see Fig. 6 in Raman *et al.*, 1986; Miller unpub. data). Furthermore, zones of iron formation not cut by the Proterozoic structures are not enriched in gold.

In this example, the possibility of low-grade, syngenetic proto-ore in the iron formation being enriched by Proterozoic strain may be applicable. However, on a regional level, intrabasement detachments could have served as fluid conduits and provided local zones of dilation for alteration and mineralization, independent of host lithology (see Sibson *et al.*, 1988). Thus such detachments are considered first order exploration targets.

SHALLOW-LEVEL DETACHMENT SURFACES

There is a limit to the thickness of rock that can undergo concentric folding. A geometric consequence is that local detachments (and/or disharmonic folds) form to accommodate space problems in constricted hinge zones (eg. fault 3, section D-D", Fig. 5; see Price, 1965; Figure 31 in Dahlstrom, 1970). Thus shallow-level detachments can form within Archean rocks due to folding of basement with cover during Proterozoic strain.

Figure 12 is a cross section from Otter Lake south to the 61 st parallel and is an interpretation of regional mapping by Eade (1974) and detailed mapping by Miller (unpub. data) of a gold prospect south of the unnamed lake south of Otter Lake, informally referred to as Lothrop lake (after the person who discovered the showings in the 1940's). Gold showings (with arsenopyrite, pyrrohtite, chalcopyrite and pyrite) and gossans (pyrrohtite-chalcopyrite-pyrite bearing) within the Archean package are distributed along northeast-trending shear zones that are aligned with the axial surfaces of tight folds in Hurwitz Group quartz arenite. Furthermore, many are concentrated along the hinge zone of a Hurwitz Group anticline. The showings are within mafic volcanic rocks. It is suggested here that the correspondence of the mineralized shear zones in Archean rocks to the Proterozoic structure (particularly the Proterozoic closure) implies that the shears are examples of shallow-level basement detachment and the mineralization is genetically related to Proterozoic strain.

Thus basement detachments in the cores of Proterozoic anticlines (particularly those that are tight) are considered first order exploration targets, regardless of host lithology.

CROSS FAULTS THAT TRANSECT THE BASEMENT-COVER CONTACT

An impressive array of oblique-slip cross faults transects the basement-cover contact (Fig. 1). These faults are systematically related to the Proterozoic folds. For example, oblique-slip cross faults fan around the closure of the box fold north of Griffin Lake and around the closure of the main D2 fold, western Griffin Lake (Fig. 1), consistent with outer arc extension during D2 folding. Although not within a cross fault, the gold-bearing quartz vein at locality 16 (130 ppb Au, sample 87-11) is within the hinge zone of a Proterozoic fold adjacent to the basement-cover contact and is interpreted to have had a similar origin. As will be discussed below, the cross faults are important sites of mineralization in the Hurwitz Group. However, at the Shear Lake deposit, pyrite-gold veins spatially related to cross faults, are not only within Hurwitz quartz arenite, but also extend into Archean schists and metagreywackes to a depth of 200 m below the basement-cover contact (Miller, 1989). Although gold was not mined from these Archean rocks at Shear Lake (Miller, 1989) Proterozoic cross faults that transect the basement-cover contact are still regarded as being worthy of exploration, within basement, as well as the Hurwitz Group.

SHEAR ZONES PARALLEL TO THE BASEMENT-COVER CONTACT

Shear zones are typically developed at the basement-cover contact (see details in Aspler and Bursey, 1990). The shears reflect large-scale flexural slip of Hurwitz Group over basement during basement-cover infolding. Proterozoic strain in basement immediately below the contact is marked either by deflection of pre-existing fabrics or micro-scale cataclasis (Aspler and Bursey, 1990). Although no gold values have been

reported, the contact-parallel shears could be potential hosts and are considered second order targets.

PROTEROZOIC-HOSTED GOLD

The most significant gold showings in Proterozoic rocks of the map area are within fractures and cross faults that are genetically related to regional folds. This structural control was documented above (see Figs. 1,8, 9, 11; and Analysis of Gossans, Kinga, Watterson and Tavani Formations); two aspects are emphasized here. First, the style of mineralization is not restricted to Kinga Formation quartz arenite, such as at the Shear Lake deposit, but may be in any unit of the Hurwitz Group (eg. highest value in the Watterson Formation, locality 1). Second, the gold showings appear to be independent of rock type in adjacent basement. Raman *et al.* (1986), noting the proximity of the Shear Lake and B-zone deposits, suggested that buried Archean gold was remobilized along cross faults into fractured Kinga quartz arenite. The B-zone is considered here to have formed during Proterozoic strain (see above), but more importantly, the Hurwitz Group showings in structure-specific sites found during the present study are not associated with any particular basement rock type, and are above all three of the principal lithological packages (Fig. 1B) in basement. Thus fractures and cross faults, particularly in Proterozoic hinge zones, are considered first order exploration targets, in any unit of the Hurwitz Group, regardless of lithology in nearby basement.

A similar conclusion concerning the control of Proterozoic mineralization by favourable structures was arrived at from analysis of structural and petrographic data from the Poorfish-Windy belt (Aspler, 1989a). The principal difference between the two areas is that of structural style and metamorphic grade (resulting from the difference in structural style). In the Poorfish-Windy belt, sulphide and opaque oxide minerals grew

during and after thrust-induced metamorphism and were probably remobilized during brittle normal faulting (Aspler, 1989a).

Values from possible syngenetic (Padlei Formation paleoplacer; Hawk Hill Member paleosol) and diagenetic (Ameto Formation and Watterson Formation diagenetic pyrite) gold showings are trivial (only a few ppb; see Analysis of Gossans, above). However, above-background levels suggest that they are worthy of continued, albeit low priority, exploration.

ACKNOWLEDGMENTS

This project was supported co-operatively by: Mineral Resources Division, Geological Survey of Canada; Indian Affairs and Northern Development Canada, Geology Office, Yellowknife; and Government of the Northwest Territories, Energy Mines and Petroleum Resources Secretariat, as part of the Canada-Northwest Territories Mineral Development Agreement, 1987-1991. C. W. Jefferson and W.A. Padgham were instrumental in securing funding. Richard Lancaster is thanked for efficient sample preparation. T.L. Bursey provided able field assistance and contributed substantially to the mapping. A.R. Miller shared unpublished data from the Cullaton Mine site and from mapping at Lothrop Lake, and provided petrographic help and discussions regarding gold metallogeny in the District of Keewatin. Expediting and radio contact were by Ingrid Brooks and Gary Gurke of Treeline Lodge, Nueltin Lake. S. Safton (Suncor Inc. Calgary) is thanked for follow-up chemistry on samples from locality 1. Critical comments by A.R. Miller and J.A. Kerswill helped to improve the manuscript.

FIGURE CAPTIONS

Figure 1: **A)** Geology Hawk Hill-Griffin-Mountain Lakes area. **B)** Stratigraphic column; thicknesses are estimates based on map data, see Table 1 for sources of geochronolologic data. **C)** Location of study area, generalized after Hoffman (1989). Reduced from Aspler (1989b).

Figure 2: Sedimentation and tectonic model for Hurwitz and Kiyuk Groups, from cratonic basin to foredeep.

Figure 3: Alternate sedimentation and tectonic model in which vertical deflections are a consequence of intraplate stresses superposed on cratonic basin subsidence (see text; after Cloetingh, 1988).

Figure 4: Cross section through open, upright concentric D1 fold. Thrust 1 and minor disharmonic folds are considered space-accommodating.

Figure 5: Cross sections through open, upright, concentric D2 folds. Out of syncline thrust 3 (section D-D") repeats the basement-cover contact and probably initiated along the intrabasement intrusive-volcanic contact.

Figure 6: Regional cross section from Ducker Lake to Poorfish Lake. Geometric constraints of concentric folding suggest that shallow-level basement-cover infolding on the east is accompanied by deep-level detachment. The link between the Hawk Hill and Poorfish-Windy thrust-fold belt may be such a detachment. Archean-hosted gold at the Cullaton B-Zone may be related to Proterozoic detachment within basement.

Figure 7: Gossan localities and gold values, Hawk Hill-Griffin-Montain Lake areas. Numbered localities are those with chemical analyses. All gold values are in ppb. Only those above the detection limit (<1ppb Au) are noted (see Table II).

Figure 8: **A)** Quartz-pyrite-gold, filling joints in Kinga Formation quartz arenite, Griffin Lake (locality 4; 23 ppb Au). **B)** Incipient breccia of quartz arenite clasts (QA) cut by annealed fracture (F) in which polygonized detrital quartz grains are cemented by chlorite-hematite-pyrite fill. Plane transmitted light (locality 5, 230 ppb Au). **C)** Breccia of quartz arenite fragments cemented by specular hematite, locality 36 (460 ppb Au). **D)** Anhedral pyrite (Py) cutting across recrystallized quartz grains with deformation lamellae and micro-quartz-filled fractures. Pyrite grains are themselves microfractured indicating pyrite growth after initiation, but before end, of deformation. Transmitted light, crossed nichols. Locality 23 (53 and 80 ppb Au).

Figure 9: Joint histograms, Kinga Formation quartz arenite, Hawk Hill-Griffin-Mountain Lakes area; polar projection, 10^{o} counting interval. The joints are not regionally consistent but reflect heterogeneous strain during both D1 and D2 (see text).

Figure 10: **A)** Massive pyrite concretion, Ameto Formation. **B)** Ameto Formation siltstone; bedding (S_0) and cleavage (S_2) as indicated. Pre-strain (diagenetic ?) pyrite grains (Py) with pressure shadow quartz (Q) and chlorite (C). Dark wavy pressure solution cleavage foliae are hematite-rich. Arrow ponts to fibrous quartz in pyrite pull-apart. Transmitted light, crossed nichols, locality 20. **C)** Ameto Formation siltstone and slate. Bedding (S0) and cleavage (S2) as indicated. Anhedral diagenetic pyrite (Py) engulfs detrital grains, but are aligned along cleavage. Transmitted light, crossed nichols, locality 20.

Figure 11. A) Gold in microfractures and disseminated in pyrite; quartz-pyrite veined calcareous arkose, Watterson Formation. Reflected light, 33,160 ppb Au (locality 1). **B)** Pyrite grain with pressure-fringe quartz, Watterson Formation calcareous siltstone. Transmitted light, crossed nichols, locality 2 (64 ppb Au). **C)** Subhedral pyrite grain with microfracures filled by hematite. Tavani Formation sub-arkose. Reflected light, locality 9 (6 ppb Au).

Figure 12: Schematic cross section from Otter Lake to south of Lothrop lake. Interpretation based on data from Eade (1974) and Miller (unpub). See text for discussion.

TABLE CAPTIONS

Table I: Description and interpretation of map units, Hawk Hill-Griffin-Mountain Lakes area (Figure numbers in table refer to Aspler and Bursey, 1990).

Table II: Sample locations, petrographic data and chemical analyses (see also Figure 7 for locations).

Table III: Summary of gold values (see Table II for details).

REFERENCES CITED

ASPLER, L.B., 1989a. Analysis of gossans, exploration guides and economic evaluation, Poorfish-Windy Thrust-Fold Belt, Ennadai Lake area, District of Keewatin. Indian Affairs and Northern Development Canada Open File EGS 1989-4, 43p.

ASPLER, L. B., 1989b. Geology of the Hawk Hill-Griffin-Mountain Lakes area, District of Keewatin. Indian Affairs and Northern Development Canada Open File Map EGS 1989-22 , 1:50,000.

ASPLER, L.B., 1988. Geology of the Poorfish-Windy Thrust-Fold belt, Ennadai Lake area, District of Keewatin. Indian Affairs and Northern Development Canada Open File Map EGS 1988-9, 1:125,000.

ASPLER, L.B., AND BURSEY, 1990. Stratigraphy, sedimentation, dome and basin basement-cover infolding and implications for gold: Hawk Hill-Griffin-Mountain Lakes area, District of Keewatin. *In* Current Research Part C, The Canadian Shield, Geological Survey of Canada Paper 90-1C.

ASPLER, L.B., BURSEY, T.L., AND MILLER, A.R., 1989. Sedimentology, structure and economic geology of the Poorfish-Windy thrust-fold belt, Ennadai Lake area, District of Keewatin, and the shelf to foreland transition in the foreland of Trans Hudson Orogen. *In* Current Research Part C, The Canadian Shield. Geological Survey of Canada Paper 89-1C, p. 143-155.

BELL, R.T., 1970a, The Hurwitz Group-a prototype for deposition on metastable cratons. *In:* A.J. Baer (ed.) Symposium on basin and geosynclines of the Canadian Shield, Geological Survey of Canada Paper 70-40, p. 159-169.

BELL, R.T., 1970b, Preliminary notes on the Hurwitz Group, Padlei map area, Northwest Territories. Geological Survey of Canada Paper 69-52, 13p.

BELL, R.T., 1968. Preliminary notes on the Proterozoic Hurwitz Group, Tavani (55K) and Kaminak Lake (55L) areas, District of Keewatin. Geological Survey of Canada Paper 68-36, 17p.

BURSEY, T.L., AND ASPLER, L.B., 1990. Regional analysis of fractures in quartz arenites of the Kinga Formation (Early Proterozoic Hurwitz Group), Hawk Hill-Mountain-Griffin Lakes area, District of Keewatin, NWT: Implications for gold. *In* Program With Abstracts, Geological Survey of Canada Current Activities Forum, p. 7.

CHIARENZELLI, J.R., and MACDONALD, R., 1986. A U-Pb zircon date for the Ennadai Group. *In:* Summary of Investigations 1986, Saskatchewan Geological Survey, Saskatchewan Energy and Mines Miscellaneous Report 86-4, p. 112-113.

CLEMMEY, H., 1985. Sedimentary ore deposits. In P.J. Brenchley and B.P.J. Williams eds., Sedimentology Recent Developments and Applied Aspects, Blackwell Scientific Publications, Oxford, p. 229-247.

CLOETINGH, S., 1988. Intraplate stress: a new element in basin analysis. *In*: K. Kleinspehn and C. Paola (eds.) New Perspectives in Basin Analysis. Springer-Verlag, New York, p. 204-230.

DAHLSTROM, C.D.A., 1970. Structural geology in the Eastern margin of the Canadian Rocky Mountains. Bulletin of Canadian Petroleum Geology, 18, p. 332-406.

EADE, K.E., 1974. Geology of Kognak River area, District of Keewatin, Northwest Territories. Geological Survey of Canada Memoir 377, 66p.

EADE, K.E., and CHANDLER, F., 1975. Geology of Watterson Lake (west half) map area, District of Keewatin. Geological Survey of Canada Paper 74-64, 10p.

GOLDSTEIN, A., and MARSHAK, S., 1988. Analysis of fracture array geometry. *In*: S. Marshak and G. Mitra eds. Basic Methods of Structural Geology, Prentice-Hall, p. 249-267.

HARRIS, C.W., GIBSON, R.G., SIMPSON, C. AND ERIKSSON, K.A., 1987. Proterozoic cuspate basement-cover structure, Needle Mountains, Colorado. Geology, 15, p. 950-953.

HOFFMAN, P.F., *in press*. Subdivision of the Churchill Province and Extent of the Trans-Hudson Orogen. *In:* J.F. Lewry and M.R. Stauffer (eds.) The Early Proterozoic Trans-Hudson Orogen of North America. Geological Association of Canada Special Paper.

HOFFMAN, P.F., 1989. Precambrian geology and tectonic history of North America. *In:* A.W. Bally and A.R. Palmer, (eds), The Geology of North America- An Overview. Geological Society of America, Boulder, p.447-512.

HOFFMAN, P.F., TIRRUL, R., KING, J.E., ST-ONGE, M.R. AND LUCAS, S.B., 1988. Axial projections and modes of crustal thickening, eastern Wopmay orogen, northwest Canadian shield. *In*: S.P. Clark Jr., B.C. Burchfiel, and J. Suppe (eds.) Processes in Continental Lithospheric Deformation, Geological Society of America Special Paper 218, p. 1-19.

LAWRANCE, L.M., 1988. Behavior of gold within the weathering profile in the Yilgarn Block, Western Australia. *In* S.E. Ho and D.I. Groves eds. Advances in Understanding Precambrian Gold Deposits, Volume II, Geology Department and University Extension and The University of Western Australia, Publication 12, p. 335-352.

LAZNICKA, P., 1989. Breccias and ores. Part 1: history, organization and petrography of breccias. Ore Geology Reviews, 4, p. 315-344.

LeCHEMINANT, A.N. AND HEAMAN, L.M. *in press*. Mackenzie igneous events, Canada: Middle Proterozoic hotspot magmatism associated with ocean opening. Earth and Planetary Science Letters.

LEWRY J.F., SIBBALD, T.I.I., and SCHLEDEWITZ, D.C.P., 1985. Variation in character of Archean rocks in the western Churchill Province and its significance. *In* L.D. Ayres, P.C. Thurston, K.D. Card, and W. Weber eds. Evolution of Archean Supracrustal Sequences, Geological Association Of Canada Special Paper 28, p. 239-261.

LORD, C.S., 1953. Geological notes on southern District of Keewatin, Northwest Territories. Geological Survey of Canada Paper 53-22, 11p.

LOVERIDGE, W.D., EADE, K.E., AND SULLIVAN, R.W., 1988. Geochronological studies from Precambrian rocks from the southern District of Keewatin. Geological Survey of Canada Paper 88-18, 36p.

MILLER, A.R., 1989. Highlights of gold studies in the Churchill Structural Province, Kaminak greenstone belt and Hurwitz Group, District of Keewatin, NWT. *In:* Current Research Part C, Geological Survey of Canada Paper 89-1C, p. 127-134.

MORTENSEN, J.K., AND THORPE, R.I., 1987. U-Pb zircon ages of felsic volcanic rocks in the Kaminak Lake area, District of Keewatin. *In*: Radiogenic Age and Isotopic Studies: Report 1, Geological Survey of Canada Paper 87-2, p. 123-128.

PAGE, C.E., 1979. B-Zone deposit, Cullaton Lake, District of Keewatin, Northwest Territories. In R. D. Morton ed., Proceedings of the Gold Workshop, Yellowknife Geological Workshop Committee, p. 323-347.

PRICE, R. A. , 1965. Flathead map-area, British Columbia and Alberta. Geological Survey of Canada Memoir 336, 221p.

RAMSAY, J.G. AND HUBER, M.I., 1987. The techniques of modern structural geology, V. 2. Folds and Fractures. Academic Press, London, 462p.

RAMAN, S., KRUSE, J., AND TENNEY, D., 1986. Geology, geophysics and geochemistry of the Cullaton B-zone gold deposit, N.W.T., Canada. *In*: L.A. Clark (ed) Gold in the Western Shield, Canadian Institute of Mining and Metallurgy Special Volume 38, p. 307-321.

SIBSON, R.H., ROBERT, F., AND POULSEN, H., 1988. High-angle reverse faults, fluid-pressure cycling, and mesothermal gold-quartz deposits. Geology, 16, p. 551-555.

STAUFFER, M.R., 1984. Manikewan: an Early Proterozoic ocean in central Canada, its igneous history and orogenic closure. Precambrian Research, 25, p. 257-281.

STEWART, A.J., 1987. Fault reactivation and superimposed folding in a Proterozoic sandstone-volcanic sequence, Davenport Province, central Australia. Journal of Structural Geology, 9, p. 441-455.

YOUNG, G.M., 1988. Proterozoic plate tectonics, glaciation and iron formations. Sedimentary Geology, 58, p. 127-144.

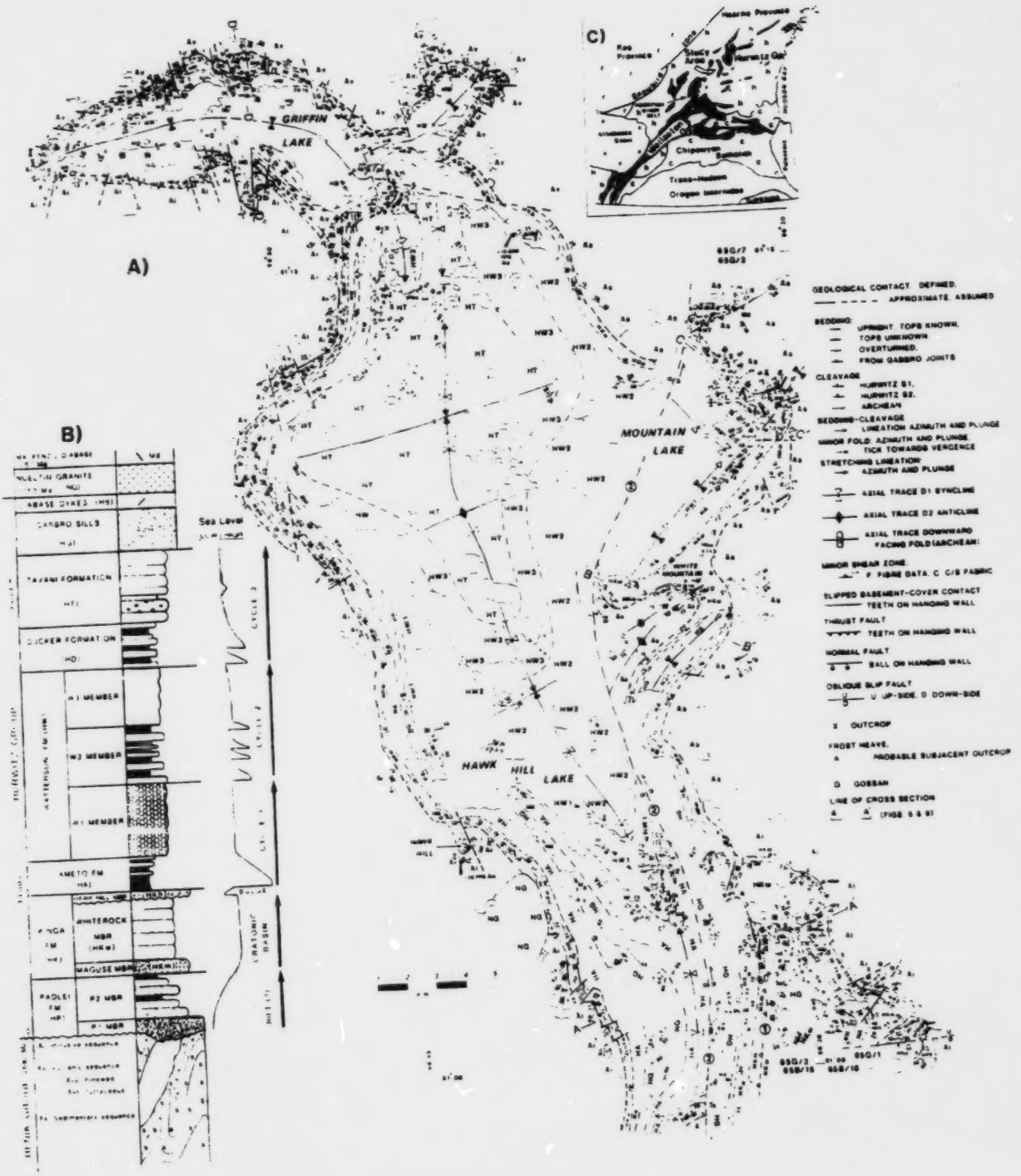
A)
B)
C)
GRIFFIN LAKE
MOUNTAIN LAKE
HAWK HILL LAKE
Sea Level
GEOLOGICAL CONTACT DEFINED.
APPROXIMATE, ASSUMED
BEDDING
UPRIGHT, TOPS KNOWN.
TOPS UNKNOWN
OVERTURNED.
FROM GABBRO JOINTS
CLEAVAGE
HURWITZ S1.
HURWITZ S2.
ARCHEAN
BEDDING-CLEAVAGE
LINEATION AZIMUTH AND PLUNGE
MINOR FOLD: AZIMUTH AND PLUNGE
TICK TOWARDS VERGENCE
STRETCHING LINEATION
AZIMUTH AND PLUNGE
AXIAL TRACE D1 SYNCLINE
AXIAL TRACE D2 ANTICLINE
AXIAL TRACE DOWNWARD FACING FOLD (ARCHEAN)
MINOR SHEAR ZONE
F FIBRE DATA, C C/S FABRIC
SLIPPED BASEMENT-COVER CONTACT
TEETH ON HANGING WALL
THRUST FAULT
TEETH ON HANGING WALL
NORMAL FAULT
BALL ON HANGING WALL
OBLIQUE SLIP FAULT
U UP-SIDE, D DOWN-SIDE
OUTCROP
FROST HEAVE.
PROBABLE SUBJACENT OUTCROP
G GOSSAN
LINE OF CROSS SECTION
(FIGS 5 & 9)
GABBRO SILLS
TAVANI FORMATION
DICKER FORMATION
M1 MEMBER
M2 MEMBER
M1 MEMBER
AMETO FM
WHITEROCK MBR
MAGUSE MBR
P2 MBR
P1 MBR
Sea Level
CYCLE 3
CYCLE 2
CYCLE 1
ERATONIT BASIN

Actual FIG 1

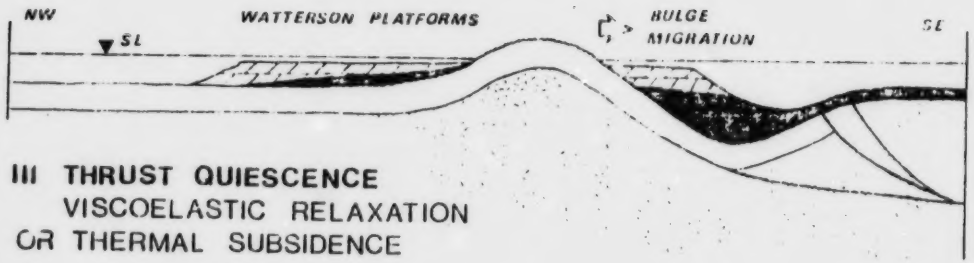

III THRUST QUIESCENCE
VISCOELASTIC RELAXATION
OR THERMAL SUBSIDENCE

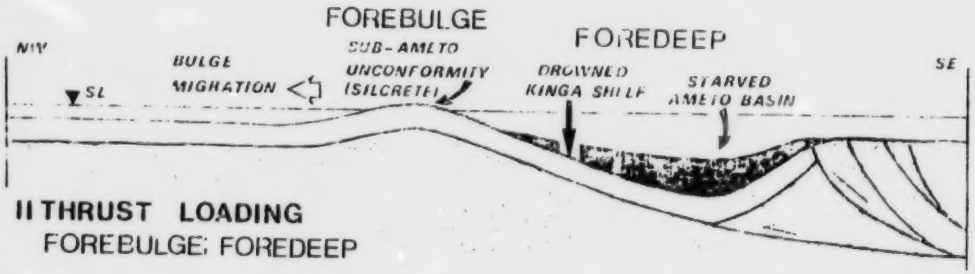

II THRUST LOADING
FOREBULGE; FOREDEEP

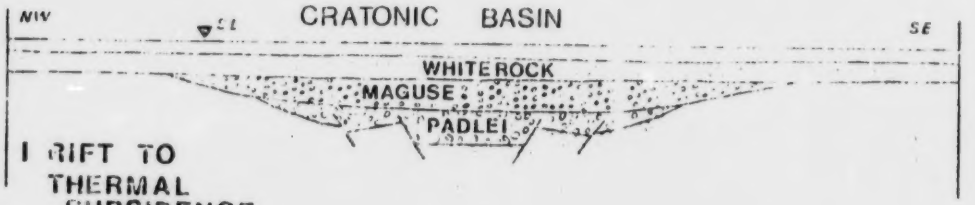

I RIFT TO
THERMAL
SUBSIDENCE

VI KIYUK DEFORMATION

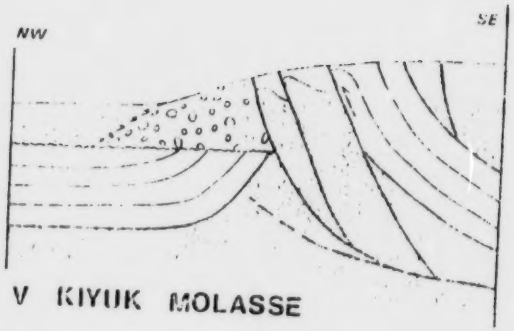

V KIYUK MOLASSE

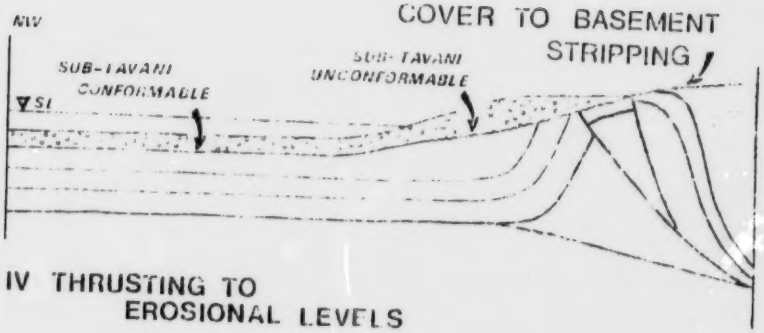

IV THRUSTING TO
EROSIONAL LEVELS

ASTEL FIG 2

INTRAPLATE STRESS CRUSTAL DEFLECTIONS

(MODIFIED AFTER CLOETINGH 1988)

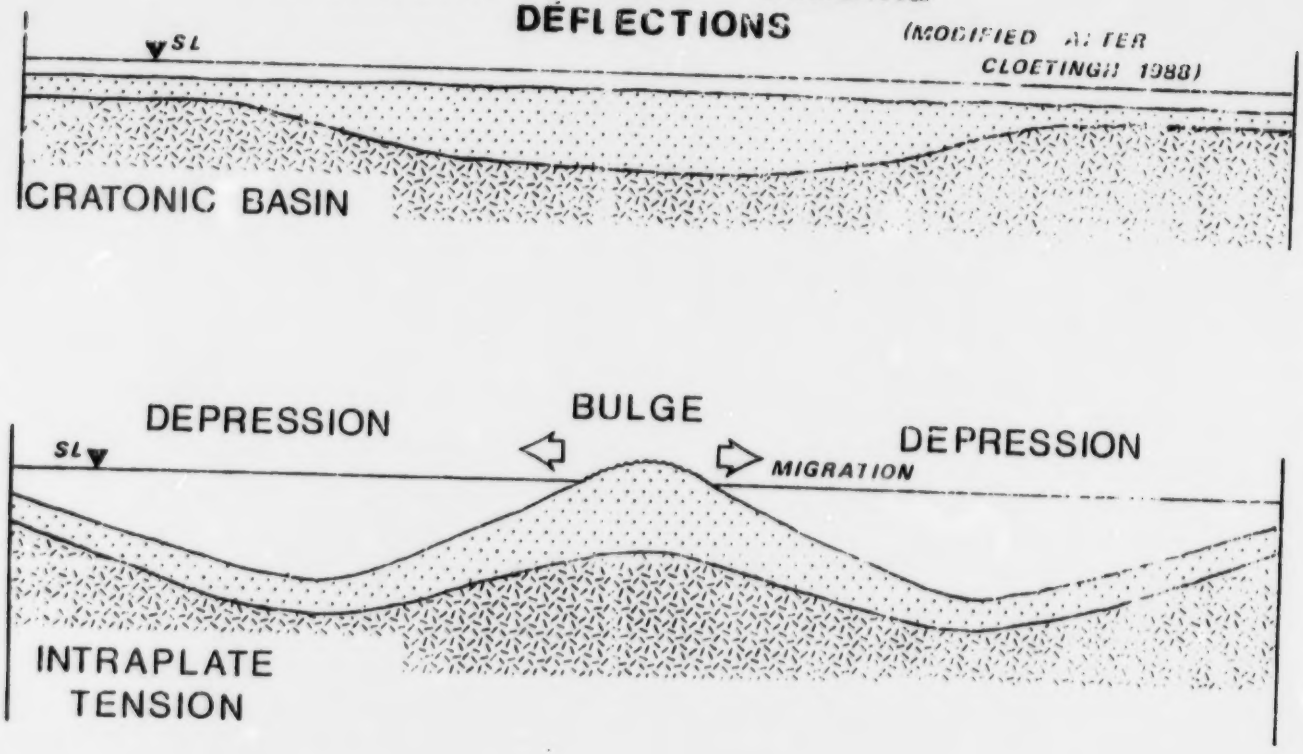

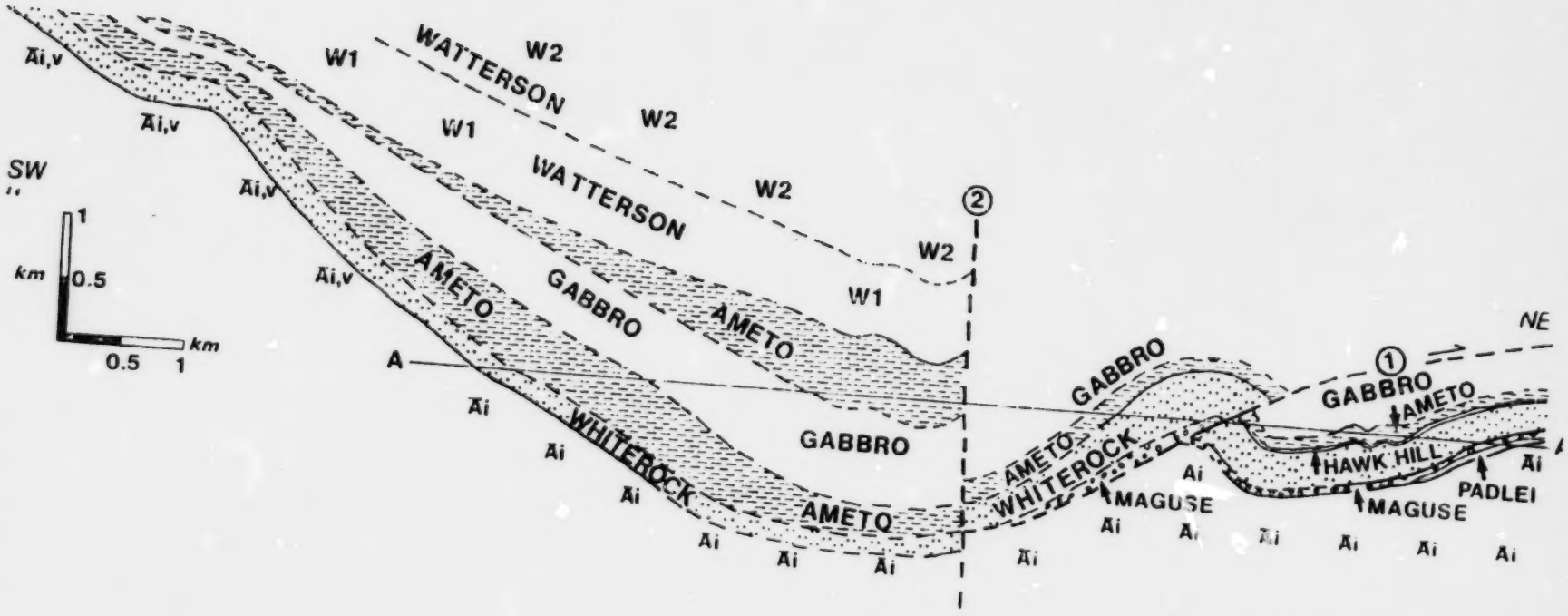
Ai,v
Ai,v
Ai,v
Ai,v
SW
1
km
0.5
0.5
1
km
W1
WATTERSON
W2
W1
WATTERSON
W2
W2
W2
W1
AMETO
GABBRO
AMETO
A
Ai
Ai
Ai
Ai
Ai
Ai
Ai
WHITEROCK
AMETO
GABBRO
AMETO
WHITEROCK
GABBRO
GABBRO
AMETO
HAWK HILL
Ai
PADLEI
Ai
MAGUSE
MAGUSE
Ai
Ai
Ai
Ai
Ai
Ai
Ai
Ai
NE
1
2

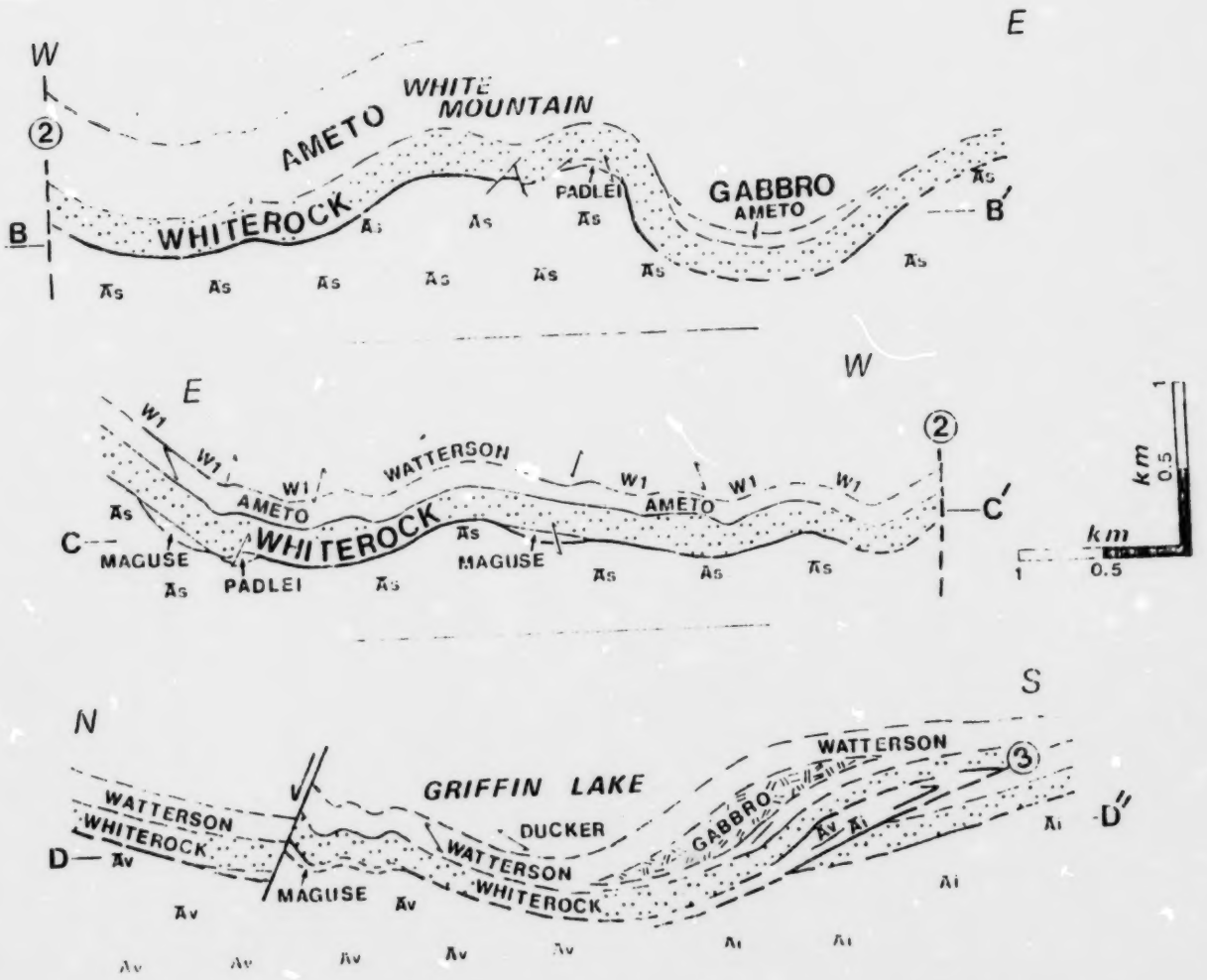
W
E
②
AMETO
WHITE MOUNTAIN
B
WHITEROCK
PADLEI
GABBRO
AMETO
B′
As
E
W
W1
WATTERSON
AMETO
C
MAGUSE
WHITEROCK
PADLEI
C′
km
0.5
1
N
S
GRIFFIN LAKE
WATTERSON
③
WHITEROCK
DUCKER
GABBRO
D
MAGUSE
D″
Av
Ai

Figure 6

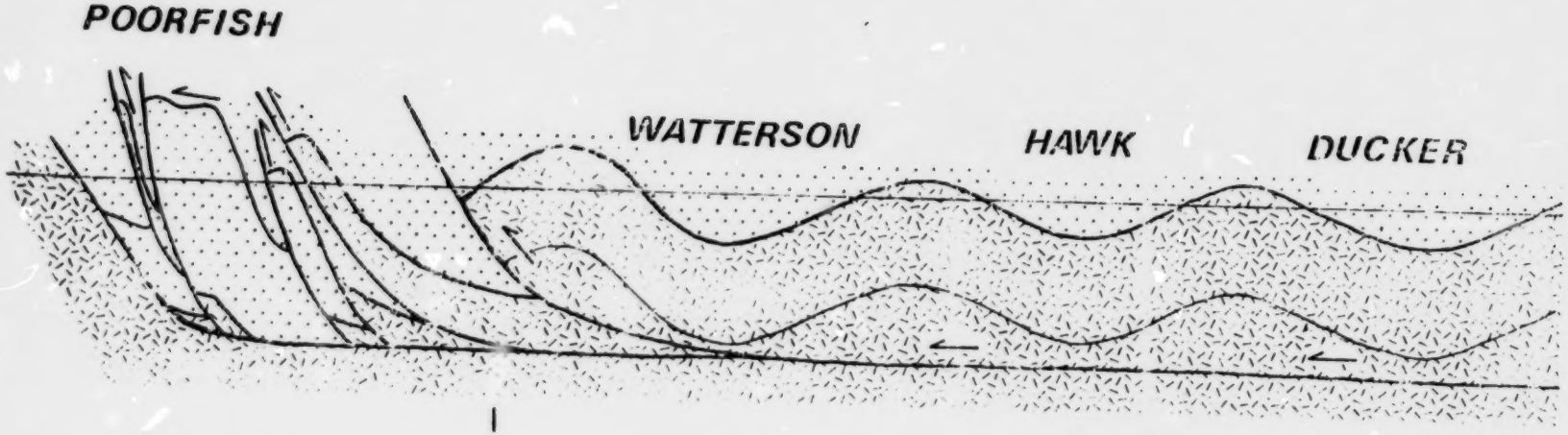
POORFISH
WATTERSON
HAWK
DUCKER
FOLD-THRUST BELT
SHALLOW-LEVEL BASEMENT COVER INFOLDING
DEEP-LEVEL DETACHMENT
15
15 km 0

GOSSAN LOCALITIES AND GOLD VALUES (in ppb)

ASPLER
FIG 7

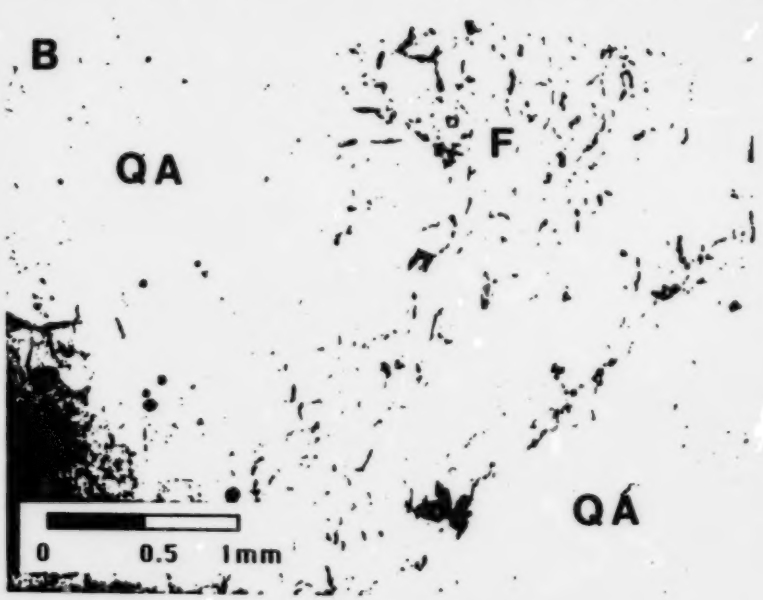

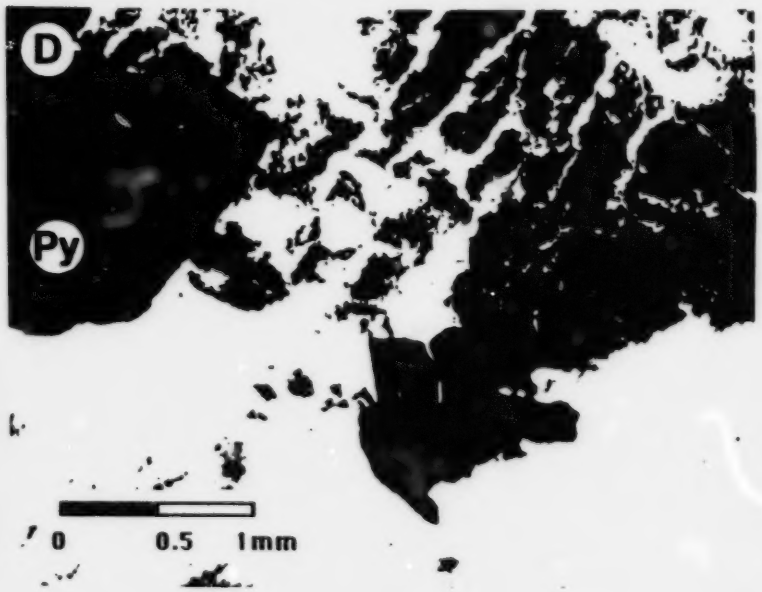

ASPLER FIG 8

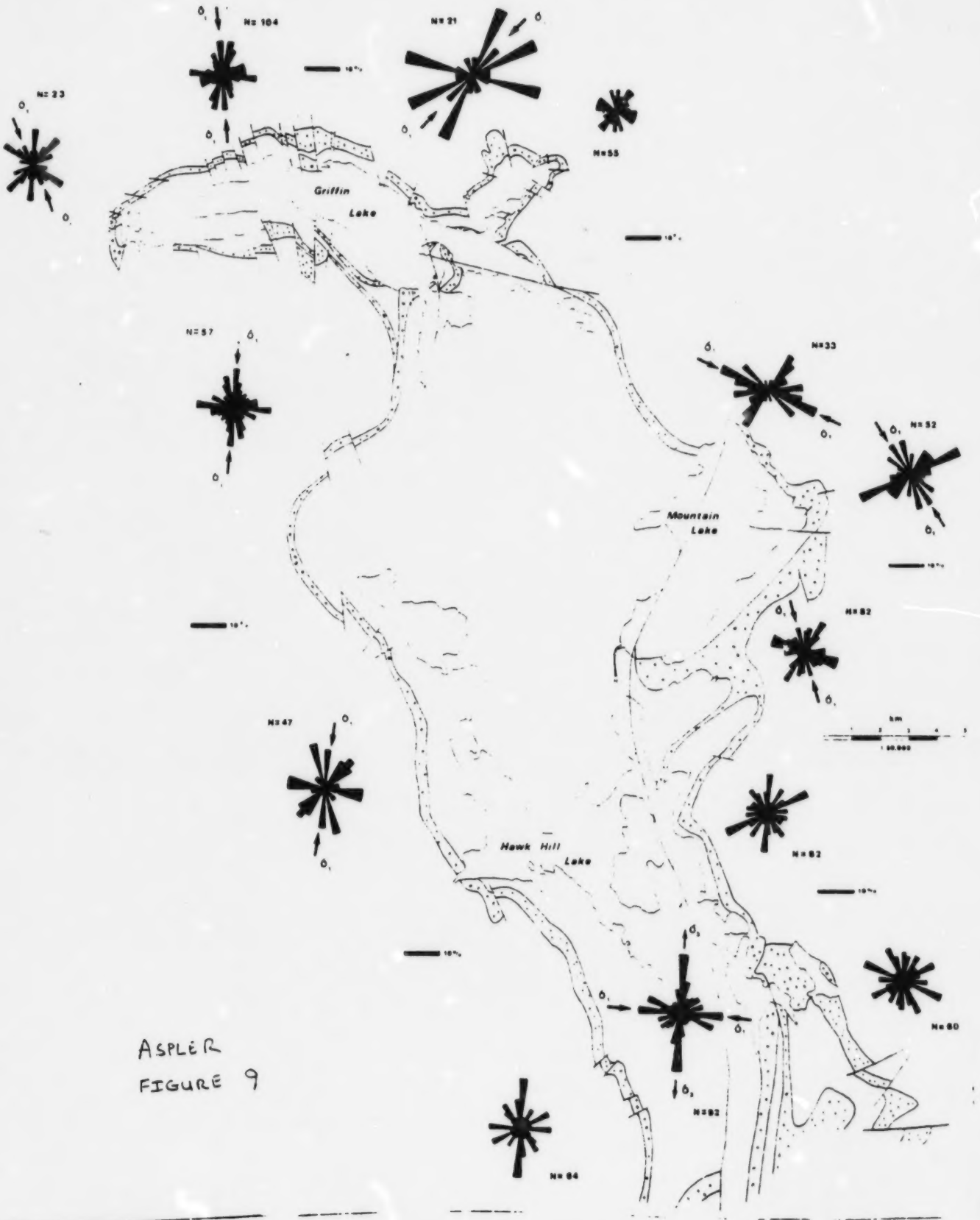

ASPLER
FIGURE 9

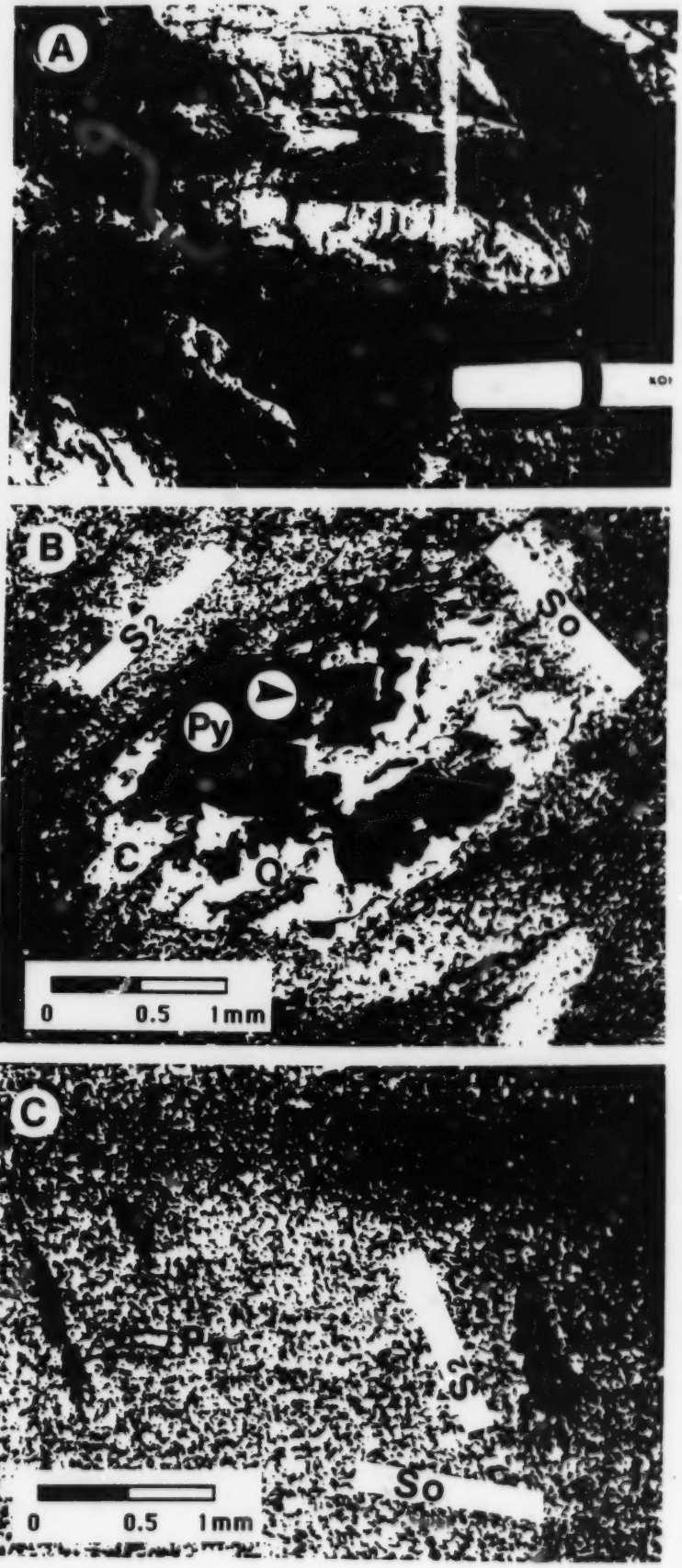

Article 10

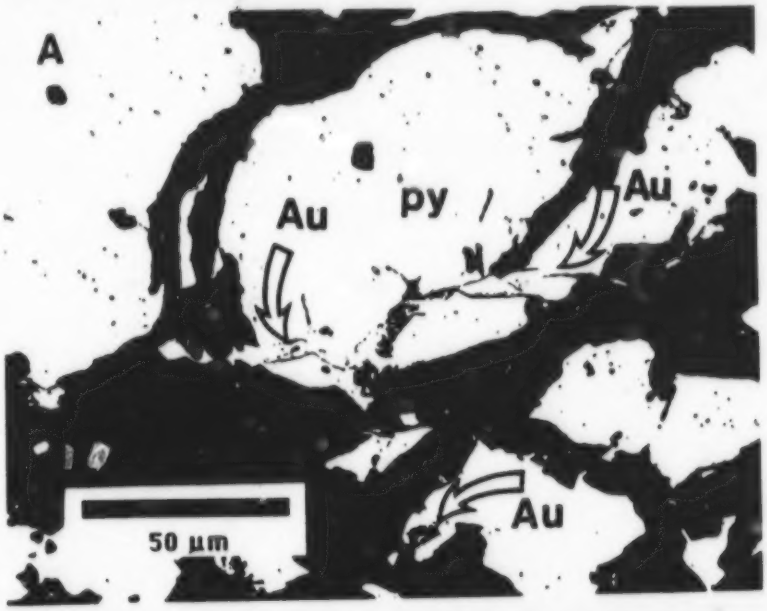

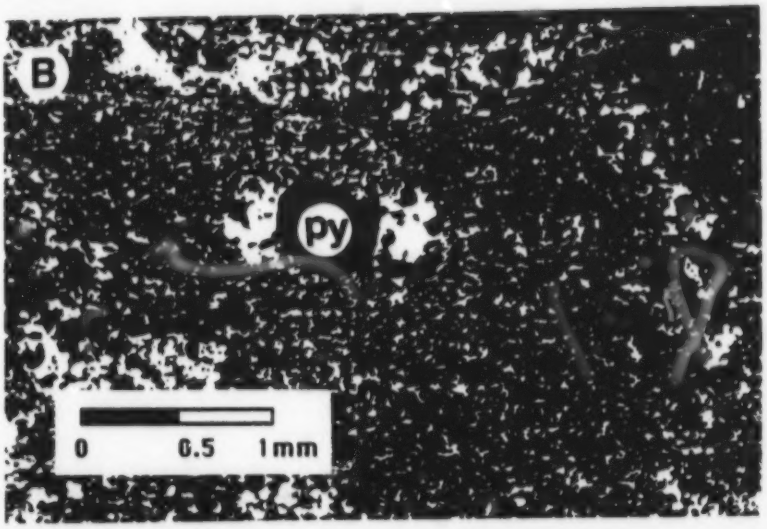

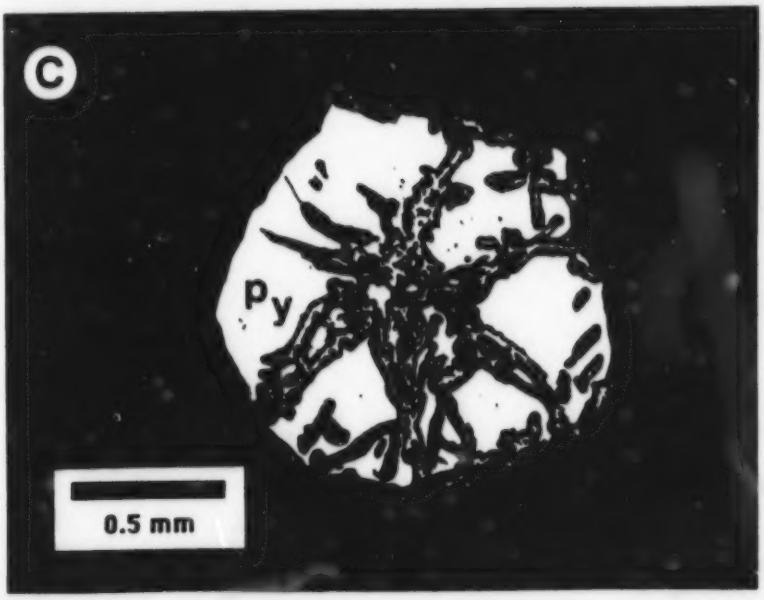

ASPLER
FIG 11

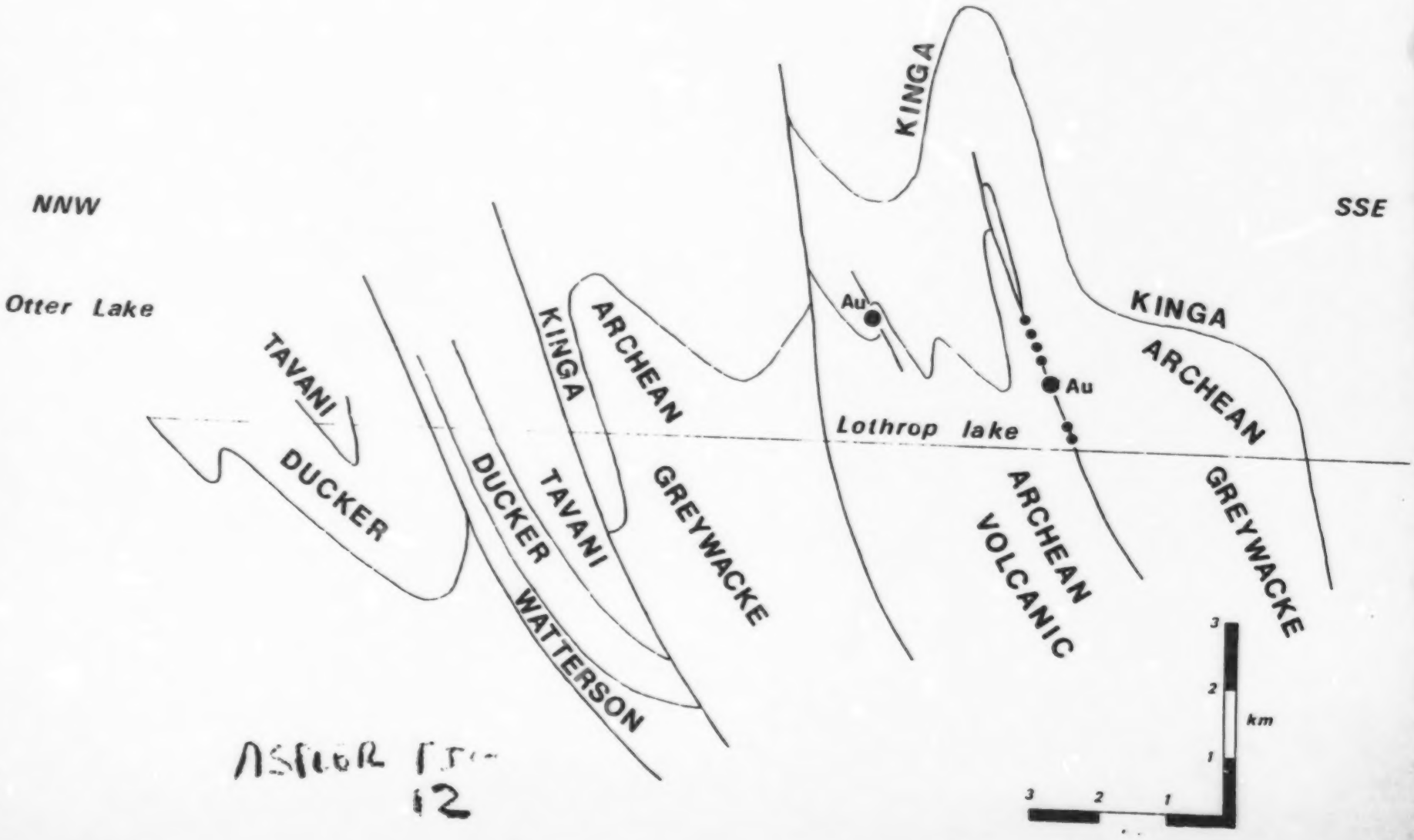
NNW
SSE
Otter Lake
TAVANI
DUCKER
KINGA
ARCHEAN
GREYWACKE
DUCKER
TAVANI
WATTERSON
KINGA
Au
Au
Lothrop lake
ARCHEAN
VOLCANIC
KINGA
ARCHEAN
GREYWACKE
3
2
1
km
3
2
1

ASTOR [illegible]
12

TABLE 1

UNIT			DESCRIPTION	INTERPRETATION	COMMENTS
					U-Pb baddeleyite 1367 ± 2 Ma (Clemmey and Badham, in press)
Mudcrack Member			Dolomitic mudstone grained, non-bedded, unstratified with sediment bed		
					U-Pb zircon 1352 ± 1.2 Ma (Hamilton et al. 1988)
Bas Bay Member			Laterally, granulometrically non-bedded		
Undivided			Fine to coarse pebbly, dolomitic clasts cutting tilted beds 3 m, following post-tilt channel or gully form. Contain reworked with internal pool, slightly rotated from bed quartz arenite	Post-tilt channel formation at Bas Bay Member	
	Ridden		Ridden silt, generally grain sandstone, coarse-grained, commonly with pebbly pockets, locally cross-bedding thereby strata. Usually well-bedded strata, plane parallel	Post-tilt channel formation at Bas Bay Member, Helsemby to Tuxen Fjord equivalent	Closely within Amelia Fm in south, absent in northern part within Wathcan Member of Ringerike
	Tuxen Fm		Tan and grey sandstone quartz arenite and siltstone with rare intervals of green shale in 1 m thick beds. Fine- to coarse-grained, locally pebbly, commonly cross-bedded, locally conglomeratic bearing clasts of pearl, arenite and carbonate floating in a quartz arenite matrix	Quartz arenites and siltstones, as shallow subtidal to subaerial deposits, typically transgressive and unconformable and unconformable conglomerates from remaining of early Cambrian adjacent sediments	Wathcan to Tuxen Member is not traceable in the map area although to the west is a basal quartz sandstone Tuxen sandstone that can also progressively distant stratigraphic levels (Bell 1976a)
	Undivided Fm		Tan to dark brown weathering quartz arenite to blue argillic clasts, beds of shale with pockets, pebbles and rippled cross-stratification. Local dimpled, reddish to orange weathering lenses	Shale was later mud flats, alternating with shallow water sandy sheets and bar deposits	Only in central and western Tuxen Fjord area, elsewhere in the map area the Wathcan Formation is unconformably overlain by the Tuxen Formation
	Wathcan Fm	W_3 W_2 W_1	Orange-weathering, rippled dolostone with tan, silver and pale interbeds Basal siltstone and carbonate as seen from 2.8 to 0.7. Carbonate member of rippled orange-weathering dolostone to thick from 50 cm to 2 m. Basal to transgressive grey shales and shale to dolostone with thin beds up of dolomite above to thick bedding-parallel tubes. Large cross-beds above to thick rhythmites, carbonate chip breccias Basal, thick and cream stromatolite, algal and oncolitic carbonate, usually bleached. Stromatolites typically have laterally linked bulbous to cabbage-like morphology. Local channel or gutter-cast with angular carbonate and quartz and rounded quartz arenite clasts rare, dm scale ripple marked sand and fine-grained siltstone	Shallow subtidal to subtidal carbonate flats with local sand deposits Shallow water fine clastic mud flats, alternating with shallow subtidal to intertidal carbonate flats. Shallowing upward sequences on 0.5 m to 1 m scale Carbonate flats with local channels with shallow water, high-energy conditions	Basal sandstone members probably equivalent to Basal Member (Hall 1976) of Mt. Wathcan Lake Area
	Amelia Fm		At base, red, blue green shale with local cream to pink pyrolitic siltstone beds. Above, alternating with thin shale, finely laminated, cross-stratified sandstone to fine beds. Fig. 4D and 4E, and 4F, and 4G, and 4H, and 4I, and 4J, and 4K, and 4L, and 4M, and 4N, and 4O, and 4P, and 4Q, and 4R, and 4S, and 4T, and 4U, and 4V, and 4W, and 4X, and 4Y, and 4Z, and 4AA, and 4AB, and 4AC, and 4AD, and 4AE, and 4AF, and 4AG, and 4AH, and 4AI, and 4AJ, and 4AK, and 4AL, and 4AM, and 4AN, and 4AO, and 4AP, and 4AQ, and 4AR, and 4AS, and 4AT, and 4AU, and 4AV, and 4AW, and 4AX, and 4AY, and 4AZ, and 4BA, and 4BB, and 4BC, and 4BD, and 4BE, and 4BF, and 4BG, and 4BH, and 4BI, and 4BJ, and 4BK, and 4BL, and 4BM, and 4BN, and 4BO, and 4BP, and 4BQ, and 4BR, and 4BS, and 4BT, and 4BU, and 4BV, and 4BW, and 4BX, and 4BY, and 4BZ, and 4CA, and 4CB, and 4CC, and 4CD, and 4CE, and 4CF, and 4CG, and 4CH, and 4CI, and 4CJ, and 4CK, and 4CL, and 4CM, and 4CN, and 4CO, and 4CP, and 4CQ, and 4CR, and 4CS, and 4CT, and 4CU, and 4CV, and 4CW, and 4CX, and 4CY, and 4CZ, and 4DA, and 4DB, and 4DC, and 4DD, and 4DE, and 4DF, and 4DG, and 4DH, and 4DI, and 4DJ, and 4DK, and 4DL, and 4DM, and 4DN, and 4DO, and 4DP, and 4DQ, and 4DR, and 4DS, and 4DT, and 4DU, and 4DV, and 4DW, and 4DX, and 4DY, and 4DZ, and 4EA, and 4EB, and 4EC, and 4ED, and 4EE, and 4EF, and 4EG, and 4EH, and 4EI, and 4EJ, and 4EK, and 4EL, and 4EM, and 4EN, and 4EO, and 4EP, and 4EQ, and 4ER, and 4ES, and 4ET, and 4EU, and 4EV, and 4EW, and 4EX, and 4EY, and 4EZ, and 4FA, and 4FB, and 4FC, and 4FD, and 4FE, and 4FF, and 4FG, and 4FH, and 4FI, and 4FJ, and 4FK, and 4FL, and 4FM, and 4FN, and 4FO, and 4FP, and 4FQ, and 4FR, and 4FS, and 4FT, and 4FU, and 4FV, and 4FW, and 4FX, and 4FY, and 4FZ, and 4GA, and 4GB, and 4GC, and 4GD, and 4GE, and 4GF, and 4GG, and 4GH, and 4GI, and 4GJ, and 4GK, and 4GL, and 4GM, and 4GN, and 4GO, and 4GP, and 4GQ, and 4GR, and 4GS, and 4GT, and 4GU, and 4GV, and 4GW, and 4GX, and 4GY, and 4GZ, and 4HA, and 4HB, and 4HC, and 4HD, and 4HE, and 4HF, and 4HG, and 4HH, and 4HI, and 4HJ, and 4HK, and 4HL, and 4HM, and 4HN, and 4HO, and 4HP, and 4HQ, and 4HR, and 4HS, and 4HT, and 4HU, and 4HV, and 4HW, and 4HX, and 4HY, and 4HZ, and 4IA, and 4IB, and 4IC, and 4ID, and 4IE, and 4IF, and 4IG, and 4IH, and 4II, and 4IJ, and 4IK, and 4IL, and 4IM, and 4IN, and 4IO, and 4IP, and 4IQ, and 4IR, and 4IS, and 4IT, and 4IU, and 4IV, and 4IW, and 4IX, and 4IY, and 4IZ, and 4JA, and 4JB, and 4JC, and 4JD, and 4JE, and 4JF, and 4JG, and 4JH, and 4JI, and 4JJ, and 4JK, and 4JL, and 4JM, and 4JN, and 4JO, and 4JP, and 4JQ, and 4JR, and 4JS, and 4JT, and 4JU, and 4JV, and 4JW, and 4JX, and 4JY, and 4JZ, and 4KA, and 4KB, and 4KC, and 4KD, and 4KE, and 4KF, and 4KG, and 4KH, and 4KI, and 4KJ, and 4KK, and 4KL, and 4KM, and 4KN, and 4KO, and 4KP, and 4KQ, and 4KR, and 4KS, and 4KT, and 4KU, and 4KV, and 4KW, and 4KX, and 4KY, and 4KZ, and 4LA, and 4LB, and 4LC, and 4LD, and 4LE, and 4LF, and 4LG, and 4LH, and 4LI, and 4LJ, and 4LK, and 4LL, and 4LM, and 4LN, and 4LO, and 4LP, and 4LQ, and 4LR, and 4LS, and 4LT, and 4LU, and 4LV, and 4LW, and 4LX, and 4LY, and 4LZ, and 4MA, and 4MB, and 4MC, and 4MD, and 4ME, and 4MF, and 4MG, and 4MH, and 4MI, and 4MJ, and 4MK, and 4ML, and 4MM, and 4MN, and 4MO, and 4MP, and 4MQ, and 4MR, and 4MS, and 4MT, and 4MU, and 4MV, and 4MW, and 4MX, and 4MY, and 4MZ, and 4NA, and 4NB, and 4NC, and 4ND, and 4NE, and 4NF, and 4NG, and 4NH, and 4NI, and 4NJ, and 4NK, and 4NL, and 4NM, and 4NN, and 4NO, and 4NP, and 4NQ, and 4NR, and 4NS, and 4NT, and 4NU, and 4NV, and 4NW, and 4NX, and 4NY, and 4NZ, and 4OA, and 4OB, and 4OC, and 4OD, and 4OE, and 4OF, and 4OG, and 4OH, and 4OI, and 4OJ, and 4OK, and 4OL, and 4OM, and 4ON, and 4OO, and 4OP, and 4OQ, and 4OR, and 4OS, and 4OT, and 4OU, and 4OV, and 4OW, and 4OX, and 4OY, and 4OZ, and 4PA, and 4PB, and 4PC, and 4PD, and 4PE, and 4PF, and 4PG, and 4PH, and 4PI, and 4PJ, and 4PK, and 4PL, and 4PM, and 4PN, and 4PO, and 4PP, and 4PQ, and 4PR, and 4PS, and 4PT, and 4PU, and 4PV, and 4PW, and 4PX, and 4PY, and 4PZ, and 4QA, and 4QB, and 4QC, and 4QD, and 4QE, and 4QF, and 4QG, and 4QH, and 4QI, and 4QJ, and 4QK, and 4QL, and 4QM, and 4QN, and 4QO, and 4QP, and 4QQ, and 4QR, and 4QS, and 4QT, and 4QU, and 4QV, and 4QW, and 4QX, and 4QY, and 4QZ, and 4RA, and 4RB, and 4RC, and 4RD, and 4RE, and 4RF, and 4RG, and 4RH, and 4RI, and 4RJ, and 4RK, and 4RL, and 4RM, and 4RN, and 4RO, and 4RP, and 4RQ, and 4RR, and 4RS, and 4RT, and 4RU, and 4RV, and 4RW, and 4RX, and 4RY, and 4RZ, and 4SA, and 4SB, and 4SC, and 4SD, and 4SE, and 4SF, and 4SG, and 4SH, and 4SI, and 4SJ, and 4SK, and 4SL, and 4SM, and 4SN, and 4SO, and 4SP, and 4SQ, and 4SR, and 4SS, and 4ST, and 4SU, and 4SV, and 4SW, and 4SX, and 4SY, and 4SZ, and 4TA, and 4TB, and 4TC, and 4TD, and 4TE, and 4TF, and 4TG, and 4TH, and 4TI, and 4TJ, and 4TK, and 4TL, and 4TM, and 4TN, and 4TO, and 4TP, and 4TQ, and 4TR, and 4TS, and 4TT, and 4TU, and 4TV, and 4TW, and 4TX, and 4TY, and 4TZ, and 4UA, and 4UB, and 4UC, and 4UD, and 4UE, and 4UF, and 4UG, and 4UH, and 4UI, and 4UJ, and 4UK, and 4UL, and 4UM, and 4UN, and 4UO, and 4UP, and 4UQ, and 4UR, and 4US, and 4UT, and 4UU, and 4UV, and 4UW, and 4UX, and 4UY, and 4UZ, and 4VA, and 4VB, and 4VC, and 4VD, and 4VE, and 4VF, and 4VG, and 4VH, and 4VI, and 4VJ, and 4VK, and 4VL, and 4VM, and 4VN, and 4VO, and 4VP, and 4VQ, and 4VR, and 4VS, and 4VT, and 4VU, and 4VV, and 4VW, and 4VX, and 4VY, and 4VZ, and 4WA, and 4WB, and 4WC, and 4WD, and 4WE, and 4WF, and 4WG, and 4WH, and 4WI, and 4WJ, and 4WK, and 4WL, and 4WM, and 4WN, and 4WO, and 4WP, and 4WQ, and 4WR, and 4WS, and 4WT, and 4WU, and 4WV, and 4WW, and 4WX, and 4WY, and 4WZ, and 4XA, and 4XB, and 4XC, and 4XD, and 4XE, and 4XF, and 4XG, and 4XH, and 4XI, and 4XJ, and 4XK, and 4XL, and 4XM, and 4XN, and 4XO, and 4XP, and 4XQ, and 4XR, and 4XS, and 4XT, and 4XU, and 4XV, and 4XW, and 4XX, and 4XY, and 4XZ, and 4YA, and 4YB, and 4YC, and 4YD, and 4YE, and 4YF, and 4YG, and 4YH, and 4YI, and 4YJ, and 4YK, and 4YL, and 4YM, and 4YN, and 4YO, and 4YP, and 4YQ, and 4YR, and 4YS, and 4YT, and 4YU, and 4YV, and 4YW, and 4YX, and 4YY, and 4YZ, and 4ZA, and 4ZB, and 4ZC, and 4ZD, and 4ZE, and 4ZF, and 4ZG, and 4ZH, and 4ZI, and 4ZJ, and 4ZK, and 4ZL, and 4ZM, and 4ZN, and 4ZO, and 4ZP, and 4ZQ, and 4ZR, and 4ZS, and 4ZT, and 4ZU, and 4ZV, and 4ZW, and 4ZX, and 4ZY, and 4ZZ, and 5AA, and 5AB, and 5AC, and 5AD, and 5AE, and 5AF, and 5AG, and 5AH, and 5AI, and 5AJ, and 5AK, and 5AL, and 5AM, and 5AN, and 5AO, and 5AP, and 5AQ, and 5AR, and 5AS, and 5AT, and 5AU, and 5AV, and 5AW, and 5AX, and 5AY, and 5AZ, and 5BA, and 5BB, and 5BC, and 5BD, and 5BE, and 5BF, and 5BG, and 5BH, and 5BI, and 5BJ, and 5BK, and 5BL, and 5BM, and 5BN, and 5BO, and 5BP, and 5BQ, and 5BR, and 5BS, and 5BT, and 5BU, and 5BV, and 5BW, and 5BX, and 5BY, and 5BZ, and 5CA, and 5CB, and 5CC, and 5CD, and 5CE, and 5CF, and 5CG, and 5CH, and 5CI, and 5CJ, and 5CK, and 5CL, and 5CM, and 5CN, and 5CO, and 5CP, and 5CQ, and 5CR, and 5CS, and 5CT, and 5CU, and 5CV, and 5CW, and 5CX, and 5CY, and 5CZ, and 5DA, and 5DB, and 5DC, and 5DD, and 5DE, and 5DF, and 5DG, and 5DH, and 5DI, and 5DJ, and 5DK, and 5DL, and 5DM, and 5DN, and 5DO, and 5DP, and 5DQ, and 5DR, and 5DS, and 5DT, and 5DU, and 5DV, and 5DW, and 5DX, and 5DY, and 5DZ, and 5EA, and 5EB, and 5EC, and 5ED, and 5EE, and 5EF, and 5EG, and 5EH, and 5EI, and 5EJ, and 5EK, and 5EL, and 5EM, and 5EN, and 5EO, and 5EP, and 5EQ, and 5ER, and 5ES, and 5ET, and 5EU, and 5EV, and 5EW, and 5EX, and 5EY, and 5EZ, and 5FA, and 5FB, and 5FC, and 5FD, and 5FE, and 5FF, and 5FG, and 5FH, and 5FI, and 5FJ, and 5FK, and 5FL, and 5FM, and 5FN, and 5FO, and 5FP, and 5FQ, and 5FR, and 5FS, and 5FT, and 5FU, and 5FV, and 5FW, and 5FX, and 5FY, and 5FZ, and 5GA, and 5GB, and 5GC, and 5GD, and 5GE, and 5GF, and 5GG, and 5GH, and 5GI, and 5GJ, and 5GK, and 5GL, and 5GM, and 5GN, and 5GO, and 5GP, and 5GQ, and 5GR, and 5GS, and 5GT, and 5GU, and 5GV, and 5GW, and 5GX, and 5GY, and 5GZ, and 5HA, and 5HB, and 5HC, and 5HD, and 5HE, and 5HF, and 5HG, and 5HH, and 5HI, and 5HJ, and 5HK, and 5HL, and 5HM, and 5HN, and 5HO, and 5HP, and 5HQ, and 5HR, and 5HS, and 5HT, and 5HU, and 5HV, and 5HW, and 5HX, and 5HY, and 5HZ, and 5IA, and 5IB, and 5IC, and 5ID, and 5IE, and 5IF, and 5IG, and 5IH, and 5II, and 5IJ, and 5IK, and 5IL, and 5IM, and 5IN, and 5IO, and 5IP, and 5IQ, and 5IR, and 5IS, and 5IT, and 5IU, and 5IV, and 5IW, and 5IX, and 5IY, and 5IZ, and 5JA, and 5JB, and 5JC, and 5JD, and 5JE, and 5JF, and 5JG, and 5JH, and 5JI, and 5JJ, and 5JK, and 5JL, and 5JM, and 5JN, and 5JO, and 5JP, and 5JQ, and 5JR, and 5JS, and 5JT, and 5JU, and 5JV, and 5JW, and 5JX, and 5JY, and 5JZ, and 5KA, and 5KB, and 5KC, and 5KD, and 5KE, and 5KF, and 5KG, and 5KH, and 5KI, and 5KJ, and 5KK, and 5KL, and 5KM, and 5KN, and 5KO, and 5KP, and 5KQ, and 5KR, and 5KS, and 5KT, and 5KU, and 5KV, and 5KW, and 5KX, and 5KY, and 5KZ, and 5LA, and 5LB, and 5LC, and 5LD, and 5LE, and 5LF, and 5LG, and 5LH, and 5LI, and 5LJ, and 5LK, and 5LL, and 5LM, and 5LN, and 5LO, and 5LP, and 5LQ, and 5LR, and 5LS, and 5LT, and 5LU, and 5LV, and 5LW, and 5LX, and 5LY, and 5LZ, and 5MA, and 5MB, and 5MC, and 5MD, and 5ME, and 5MF, and 5MG, and 5MH, and 5MI, and 5MJ, and 5MK, and 5ML, and 5MM, and 5MN, and 5MO, and 5MP, and 5MQ, and 5MR, and 5MS, and 5MT, and 5MU, and 5MV, and 5MW, and 5MX, and 5MY, and 5MZ, and 5NA, and 5NB, and 5NC, and 5ND, and 5NE, and 5NF, and 5NG, and 5NH, and 5NI, and 5NJ, and 5NK, and 5NL, and 5NM, and 5NN, and 5NO, and 5NP, and 5NQ, and 5NR, and 5NS, and 5NT, and 5NU, and 5NV, and 5NW, and 5NX, and 5NY, and 5NZ, and 5OA, and 5OB, and 5OC, and 5OD, and 5OE, and 5OF, and 5OG, and 5OH, and 5OI, and 5OJ, and 5OK, and 5OL, and 5OM, and 5ON, and 5OO, and 5OP, and 5OQ, and 5OR, and 5OS, and 5OT, and 5OU, and 5OV, and 5OW, and 5OX, and 5OY, and 5OZ, and 5PA, and 5PB, and 5PC, and 5PD, and 5PE, and 5PF, and 5PG, and 5PH, and 5PI, and 5PJ, and 5PK, and 5PL, and 5PM, and 5PN, and 5PO, and 5PP, and 5PQ, and 5PR, and 5PS, and 5PT, and 5PU, and 5PV, and 5PW, and 5PX, and 5PY, and 5PZ, and 5QA, and 5QB, and 5QC, and 5QD, and 5QE, and 5QF, and 5QG, and 5QH, and 5QI, and 5QJ, and 5QK, and 5QL, and 5QM, and 5QN, and 5QO, and 5QP, and 5QQ, and 5QR, and 5QS, and 5QT, and 5QU, and 5QV, and 5QW, and 5QX, and 5QY, and 5QZ, and 5RA, and 5RB, and 5RC, and 5RD, and 5RE, and 5RF, and 5RG, and 5RH, and 5RI, and 5RJ, and 5RK, and 5RL, and 5RM, and 5RN, and 5RO, and 5RP, and 5RQ, and 5RR, and 5RS, and 5RT, and 5RU, and 5RV, and 5RW, and 5RX, and 5RY, and 5RZ, and 5SA, and 5SB, and 5SC, and 5SD, and 5SE, and 5SF, and 5SG, and 5SH, and 5SI, and 5SJ, and 5SK, and 5SL, and 5SM, and 5SN, and 5SO, and 5SP, and 5SQ, and 5SR, and 5SS, and 5ST, and 5SU, and 5SV, and 5SW, and 5SX, and 5SY, and 5SZ, and 5TA, and 5TB, and 5TC, and 5TD, and 5TE, and 5TF, and 5TG, and 5TH, and 5TI, and 5TJ, and 5TK, and 5TL, and 5TM, and 5TN, and 5TO, and 5TP, and 5TQ, and 5TR, and 5TS, and 5TT, and 5TU, and 5TV, and 5TW, and 5TX, and 5TY, and 5TZ, and 5UA, and 5UB, and 5UC, and 5UD, and 5UE, and 5UF, and 5UG, and 5UH, and 5UI, and 5UJ, and 5UK, and 5UL, and 5UM, and 5UN, and 5UO, and 5UP, and 5UQ, and 5UR, and 5US, and 5UT, and 5UU, and 5UV, and 5UW, and 5UX, and 5UY, and 5UZ, and 5VA, and 5VB, and 5VC, and 5VD, and 5VE, and 5VF, and 5VG, and 5VH, and 5VI, and 5VJ, and 5VK, and 5VL, and 5VM, and 5VN, and 5VO, and 5VP, and 5VQ, and 5VR, and 5VS, and 5VT, and 5VU, and 5VV, and 5VW, and 5VX, and 5VY, and 5VZ, and 5WA, and 5WB, and 5WC, and 5WD, and 5WE, and 5WF, and 5WG, and 5WH, and 5WI, and 5WJ, and 5WK, and 5WL, and 5WM, and 5WN, and 5WO, and 5WP, and 5WQ, and 5WR, and 5WS, and 5WT, and 5WU, and 5WV, and 5WW, and 5WX, and 5WY, and 5WZ, and 5XA, and 5XB, and 5XC, and 5XD, and 5XE, and 5XF, and 5XG, and 5XH, and 5XI, and 5XJ, and 5XK, and 5XL, and 5XM, and 5XN, and 5XO, and 5XP, and 5XQ, and 5XR, and 5XS, and 5XT, and 5XU, and 5XV, and 5XW, and 5XX, and 5XY, and 5XZ, and 5YA, and 5YB, and 5YC, and 5YD, and 5YE, and 5YF, and 5YG, and 5YH, and 5YI, and 5YJ, and 5YK, and 5YL, and 5YM, and 5YN, and 5YO, and 5YP, and 5YQ, and 5YR, and 5YS, and 5YT, and 5YU, and 5YV, and 5YW, and 5YX, and 5YY, and 5YZ, and 5ZA, and 5ZB, and 5ZC, and 5ZD, and 5ZE, and 5ZF, and 5ZG, and 5ZH, and 5ZI, and 5ZJ, and 5ZK, and 5ZL, and 5ZM, and 5ZN, and 5ZO, and 5ZP, and 5ZQ, and 5ZR, and 5ZS, and 5ZT, and 5ZU, and 5ZV, and 5ZW, and 5ZX, and 5ZY, and 5ZZ, and 6AA, and 6AB, and 6AC, and 6AD, and 6AE, and 6AF, and 6AG, and 6AH, and 6AI, and 6AJ, and 6AK, and 6AL, and 6AM, and 6AN, and 6AO, and 6AP, and 6AQ, and 6AR, and 6AS, and 6AT, and 6AU, and 6AV, and 6AW, and 6AX, and 6AY, and 6AZ, and 6BA, and 6BB, and 6BC, and 6BD, and 6BE, and 6BF, and 6BG, and 6BH, and 6BI, and 6BJ, and 6BK, and 6BL, and 6BM, and 6BN, and 6BO, and 6BP, and 6BQ, and 6BR, and 6BS, and 6BT, and 6BU, and 6BV, and 6BW, and 6BX, and 6BY, and 6BZ, and 6CA, and 6CB, and 6CC, and 6CD, and 6CE, and 6CF, and 6CG, and 6CH, and 6CI, and 6CJ, and 6CK, and 6CL, and 6CM, and 6CN, and 6CO, and 6CP, and 6CQ, and 6CR, and 6CS, and 6CT, and 6CU, and 6CV, and 6CW, and 6CX, and 6CY, and 6CZ, and 6DA, and 6DB, and 6DC, and 6DD, and 6DE, and 6DF, and 6DG, and 6DH, and 6DI, and 6DJ, and 6DK, and 6DL, and 6DM, and 6DN, and 6DO, and 6DP, and 6DQ, and 6DR, and 6DS, and 6DT, and 6DU, and 6DV, and 6DW, and 6DX, and 6DY, and 6DZ, and 6EA, and 6EB, and 6EC, and 6ED, and 6EE, and 6EF, and 6EG, and 6EH, and 6EI, and 6EJ, and 6EK, and 6EL, and 6EM, and 6EN, and 6EO, and 6EP, and 6EQ, and 6ER, and 6ES, and 6ET, and 6EU, and 6EV, and 6EW, and 6EX, and 6EY, and 6EZ, and 6FA, and 6FB, and 6FC, and 6FD, and 6FE, and 6FF, and 6FG, and 6FH, and 6FI, and 6FJ, and 6FK, and 6FL, and 6FM, and 6FN, and 6FO, and 6FP, and 6FQ, and 6FR, and 6FS, and 6FT, and 6FU, and 6FV, and 6FW, and 6FX, and 6FY, and 6FZ, and 6GA, and 6GB, and 6GC, and 6GD, and 6GE, and 6GF, and 6GG, and 6GH, and 6GI, and 6GJ, and 6GK, and 6GL, and 6GM, and 6GN, and 6GO, and 6GP, and 6GQ, and 6GR, and 6GS, and 6GT, and 6GU, and 6GV, and 6GW, and 6GX, and 6GY, and 6GZ, and 6HA, and 6HB, and 6HC, and 6HD, and 6HE, and 6HF, and 6HG, and 6HH, and 6HI, and 6HJ, and 6HK, and 6HL, and 6HM, and 6HN, and 6HO, and 6HP, and 6HQ, and 6HR, and 6HS, and 6HT, and 6HU, and 6HV, and 6HW, and 6HX, and 6HY, and 6HZ, and 6IA, and 6IB, and 6IC, and 6ID, and 6IE, and 6IF, and 6IG, and 6IH, and 6II, and 6IJ, and 6IK, and 6IL, and 6IM, and 6IN, and 6IO, and 6IP, and 6IQ, and 6IR, and 6IS, and 6IT, and 6IU, and 6IV, and 6IW, and 6IX, and 6IY, and 6IZ, and 6JA, and 6JB, and 6JC, and 6JD, and 6JE, and 6JF, and 6JG, and 6JH, and 6JI, and 6JJ, and 6JK, and 6JL, and 6JM, and 6JN, and 6JO, and 6JP, and 6JQ, and 6JR, and 6JS, and 6JT, and 6JU, and 6JV, and 6JW, and 6JX, and 6JY, and 6JZ, and 6KA, and 6KB, and 6KC, and 6KD, and 6KE, and 6KF, and 6KG, and 6KH, and 6KI, and 6KJ, and 6KK, and 6KL, and 6KM, and 6KN, and 6KO, and 6KP, and 6KQ, and 6KR, and 6KS, and 6KT, and 6KU, and 6KV, and 6KW, and 6KX, and 6KY, and 6KZ, and 6LA, and 6LB, and 6LC, and 6LD, and 6LE, and 6LF, and 6LG, and 6LH, and 6LI, and 6LJ, and 6LK, and 6LL, and 6LM, and 6LN, and 6LO, and 6LP, and 6LQ, and 6LR, and 6LS, and 6LT, and 6LU, and 6LV, and 6LW, and 6LX, and 6LY, and 6LZ, and 6MA, and 6MB, and 6MC, and 6MD, and 6ME, and 6MF, and 6MG, and 6MH, and 6MI, and 6MJ, and 6MK, and 6ML, and 6MM, and 6MN, and 6MO, and 6MP, and 6MQ, and 6MR, and 6MS, and 6MT, and 6MU, and 6MV, and 6MW, and 6MX, and 6MY, and 6MZ, and 6NA, and 6NB, and 6NC, and 6ND, and 6NE, and 6NF, and 6NG, and 6NH, and 6NI, and 6NJ, and 6NK, and 6NL, and 6NM, and 6NN, and 6NO, and 6NP, and 6NQ, and 6NR, and 6NS, and 6NT, and 6NU, and 6NV, and 6NW, and 6NX, and 6NY, and 6NZ, and 6OA, and 6OB, and 6OC, and 6OD, and 6OE, and 6OF, and 6OG, and 6OH, and 6OI, and 6OJ, and 6OK, and 6OL, and 6OM, and 6ON, and 6OO, and 6OP, and 6OQ, and 6OR, and 6OS, and 6OT, and 6OU, and 6OV, and 6OW, and 6OX, and 6OY, and 6OZ, and 6PA, and 6PB, and 6PC, and 6PD, and 6PE, and 6PF, and 6PG, and 6PH, and 6PI, and 6PJ, and 6PK, and 6PL, and 6PM, and 6PN, and 6PO, and 6PP, and 6PQ, and 6PR, and 6PS, and 6PT, and 6PU, and 6PV, and 6PW, and 6PX, and 6PY, and 6PZ, and 6QA, and 6QB, and 6QC, and 6QD, and 6QE, and 6QF, and 6QG, and 6QH, and 6QI, and 6QJ, and 6QK, and 6QL, and 6QM, and 6QN, and 6QO, and 6QP, and 6QQ, and 6QR, and 6QS, and 6QT, and 6QU, and 6QV, and 6QW, and 6QX, and 6QY, and 6QZ, and 6RA, and 6RB, and 6RC, and 6RD, and 6RE, and 6RF, and 6RG, and 6RH, and 6RI, and 6RJ, and 6RK, and 6RL, and 6RM, and 6RN, and 6RO, and 6RP, and 6RQ, and 6RR, and 6RS, and 6RT, and 6RU, and 6RV, and 6RW, and 6RX, and 6RY, and 6RZ, and 6SA, and 6SB, and 6SC, and 6SD, and 6SE, and 6SF, and 6SG, and 6SH, and 6SI, and 6SJ, and 6SK, and 6SL, and 6SM, and 6SN, and 6SO, and 6SP, and 6SQ, and 6SR, and 6SS, and 6ST, and 6SU, and 6SV, and 6SW, and 6SX, and 6SY, and 6SZ, and 6TA, and 6TB, and 6TC, and 6TD, and 6TE, and 6TF, and 6TG, and 6TH, and 6TI, and 6TJ, and 6TK, and 6TL, and 6TM, and 6TN, and 6TO, and 6TP, and 6TQ, and 6TR, and 6TS, and 6TT, and 6TU, and 6TV, and 6TW, and 6TX, and 6TY, and 6TZ, and 6UA, and 6UB, and 6UC, and 6UD, and 6UE, and 6UF, and 6UG, and 6UH, and 6UI, and 6UJ, and 6UK, and 6UL, and 6UM, and 6UN, and 6UO, and 6UP, and 6UQ, and 6UR, and 6US, and 6UT, and 6UU, and 6UV, and 6UW, and 6UX, and 6UY, and 6UZ, and 6VA, and 6VB, and 6VC, and 6VD, and 6VE, and 6VF, and 6VG, and 6VH, and 6VI, and 6VJ, and 6VK, and 6VL, and 6VM, and 6VN, and 6VO, and 6VP, and 6VQ, and 6VR, and 6VS, and 6VT, and 6VU, and 6VV, and 6VW, and 6VX, and 6VY, and 6VZ, and 6WA, and 6WB, and 6WC, and 6WD, and 6WE, and 6WF, and 6WG, and 6WH, and 6WI, and 6WJ, and 6WK, and 6WL, and 6WM, and 6WN, and 6WO, and 6WP, and 6WQ, and 6WR, and 6WS, and 6WT, and 6WU, and 6WV, and 6WW, and 6WX, and 6WY, and 6WZ, and 6XA, and 6XB, and 6XC, and 6XD, and 6XE, and 6XF, and 6XG, and 6XH, and 6XI, and 6XJ, and 6XK, and 6XL, and 6XM, and 6XN, and 6XO, and 6XP, and 6XQ, and 6XR, and 6XS, and 6XT, and 6XU, and 6XV, and 6XW, and 6XX, and 6XY, and 6XZ, and 6YA, and 6YB, and 6YC, and 6YD, and 6YE, and 6YF, and 6YG, and 6YH, and 6YI, and 6YJ, and 6YK, and 6YL, and 6YM, and 6YN, and 6YO, and 6YP, and 6YQ, and 6YR, and 6YS, and 6YT, and 6YU, and 6YV, and 6YW, and 6YX, and 6YY, and 6YZ, and 6ZA, and 6ZB, and 6ZC, and 6ZD, and 6ZE, and 6ZF, and 6ZG, and 6ZH, and 6ZI, and 6ZJ, and 6ZK, and 6ZL, and 6ZM, and 6ZN, and 6ZO, and 6ZP, and 6ZQ, and 6ZR, and 6ZS, and 6ZT, and 6ZU, and 6ZV, and 6ZW, and 6ZX, and 6ZY, and 6ZZ, and 7AA, and 7AB, and 7AC, and 7AD, and 7AE, and 7AF, and 7AG, and 7AH, and 7AI, and 7AJ, and 7AK, and 7AL, and 7AM, and 7AN, and 7AO, and 7AP, and 7AQ, and 7AR, and 7AS, and 7AT, and 7AU, and 7AV, and 7AW, and 7AX, and 7AY, and 7AZ, and 7BA, and 7BB, and 7BC, and 7BD, and 7BE, and 7BF, and 7BG, and 7BH, and 7BI, and 7BJ, and 7BK, and 7BL, and 7BM, and 7BN, and 7BO, and 7BP, and 7BQ, and 7BR, and 7BS, and 7BT, and 7BU, and 7BV, and 7BW, and 7BX, and 7BY, and 7BZ, and 7CA, and 7CB, and 7CC, and 7CD, and 7CE, and 7CF, and 7CG, and 7CH, and 7CI, and 7CJ, and 7CK, and 7CL, and 7CM, and 7CN, and 7CO, and 7CP, and 7CQ, and 7CR, and 7CS, and 7CT, and 7CU, and 7CV, and 7CW, and 7CX, and 7CY, and 7CZ, and 7DA, and 7DB, and 7DC, and 7DD, and 7DE, and 7DF, and 7DG, and 7DH, and 7DI, and 7DJ, and 7DK, and 7DL, and 7DM, and 7DN, and 7DO, and 7DP, and 7DQ, and 7DR, and 7DS, and 7DT, and 7DU, and 7DV, and 7DW, and 7DX, and 7DY, and 7DZ, and 7EA, and 7EB, and 7EC, and 7ED, and 7EE, and 7EF, and 7EG, and 7EH, and 7EI, and 7EJ, and 7EK, and 7EL, and 7EM, and 7EN, and 7EO, and 7EP, and 7EQ, and 7ER, and 7ES, and 7ET, and 7EU, and 7EV, and 7EW, and 7EX, and 7EY, and 7EZ, and 7FA, and 7FB, and 7FC, and 7FD, and 7FE, and 7FF, and 7FG, and 7FH, and 7FI, and 7FJ, and 7FK, and 7FL, and 7FM, and 7FN, and 7FO, and 7FP, and 7FQ, and 7FR, and 7FS, and 7FT, and 7FU, and 7FV, and 7FW, and 7FX, and 7FY, and 7FZ, and 7GA, and 7GB, and 7GC, and 7GD, and 7GE, and 7GF, and 7GG, and 7GH, and 7GI, and 7GJ, and 7GK, and 7GL, and 7GM, and 7GN, and 7GO, and 7GP, and 7GQ, and 7GR, and 7GS, and 7GT, and 7GU, and 7GV, and 7GW, and 7GX, and 7GY, and 7GZ, and 7HA, and 7HB, and 7HC, and 7HD, and 7HE, and 7HF, and 7HG, and 7HH, and 7HI, and 7HJ, and 7HK, and 7HL, and 7HM, and 7HN, and 7HO, and 7HP, and 7HQ, and 7HR, and 7HS, and 7HT, and 7HU, and 7HV, and 7HW, and 7HX, and 7HY, and 7HZ, and 7IA, and 7IB, and 7IC, and 7ID, and 7IE, and 7IF, and 7IG, and 7IH, and 7II, and 7IJ, and 7IK, and 7IL, and 7IM, and 7IN, and 7IO, and 7IP, and 7IQ, and 7IR, and 7IS, and 7IT, and 7IU, and 7IV, and 7IW, and 7IX, and 7IY, and 7IZ, and 7JA, and 7JB, and 7JC, and 7JD, and 7JE, and 7JF, and 7JG, and 7JH, and 7JI, and 7JJ, and 7JK, and 7JL, and 7JM, and 7JN, and 7JO, and 7JP, and 7JQ, and 7JR, and 7JS, and 7JT, and 7JU, and 7JV, and 7JW, and 7JX, and 7JY, and 7JZ, and 7KA, and 7KB, and 7KC, and 7KD, and 7KE, and 7KF, and 7KG, and 7KH, and 7KI, and 7KJ, and 7KK, and 7KL, and 7KM, and 7KN, and 7KO, and 7KP, and 7KQ, and 7KR, and 7KS, and 7KT, and 7KU, and 7KV, and 7KW, and 7KX, and 7KY, and 7KZ, and 7LA, and 7LB, and 7LC, and 7LD, and 7LE, and 7LF, and 7LG, and 7LH, and 7LI, and 7LJ, and 7LK, and 7LL, and 7LM, and 7LN, and 7LO, and 7LP, and 7LQ, and 7LR, and 7LS, and 7LT, and 7LU, and 7LV, and 7LW, and 7LX, and 7LY, and 7LZ, and 7MA, and

TABLE II-1-A

SAMPLE	LOCALE	NTS/ UTM	UNIT	DESCRIPTION
100-11A	1	65G/7, 177915	Watterson Formation	Quartz-pyrite veined calcareous arkose. Gold fills microfractures and is disseminated in pyrite (Fig. 11 A).
100-11B	2	65G/7, 177914	Watterson Formation	Calcareous silstone. Pyrite disseminations to 2mm, with local chalcopyrite and hematite inclusions; pyrite pre-strain (diagenetic?) as indicated by carbonate-quartz pressure fringes (Fig. 11 B). Local disseminated and fracture-fill hematite.
106-3	3	65G/7, 159940	Whiterock Member	Quartz arenite with disseminated pyrite clusters to 1 cm
97-11	4	65G/7, 132924	Whiterock Member	Quartz arenite with veins of sulphides following fractures (Fig. 8 A), disseminated pyrite euhedra cut across detrital quartz boundaries.
96-2	5	65G/7, 128929	Whiterock Member	Quartz arenite with hematite and pyrite in zones of chloritic alteration along fractures; local disseminated pyrite.
97-1	6	65G/7, 123924	Whiterock Member	Quartz arenite with sulphide stains along bedding, fractures and cross-cutting quartz veins.
97-2	7	65G/7, 117924	Whiterock Member	Quartz arenite with sulphide stains along fractures and cross-cutting quartz veins; disseminated pyrite.
102-7	8	65G/7, 095937	Whiterock Member	Quartz arenite with veins of sulphides; disseminated pyrite clusters to 3 mm.
97-5A	9	65G/2, 127896	Tavani Formation	Brecciated sub-arkose with lenses of cryptalgal laminate. Pyrite disseminations to 3 mm; microfractures in pyrite filled with hematite (Fig. 11C); hematite fracture-fills.
97-5B	9	65G/2, 127896	Tavani Formation	Brecciated sub-arkose with lenses of cryptalgal laminate. Pyrite disseminations to 3 mm; microfractures in pyrite filled with hematite; hematite fracture-fills.
101-13	10	65/G2, 113891	Archean	Mafic tuff with pyrite concentrations along layering.
101-16	11	65/G2, 114890	Whiterock Member	Quartz arenite with sulphide stain along fractures

TABLE II-1-B

SAMPLE	LOCALE	NTS/ UTM	UNIT	DESCRIPTION
101-33	12	65/G2, 094872	Whiterock Member	Quartz arenite in fault contact with mafic tuff. Mylonitic layering and chloritic alteration along contact. Massive and disseminated py and cpy along layering and in cross-cutting fractures. Pyrrohtite-chalcopyrite-magnetite disseminated in pyrite
84-21	13	65/G2, 113796	Whiterock Member	Breccia of quartz arenite fragments in matrix of chloritized quartz arenite. Matrix with pyrite clusters to 1 cm, disseminated hematite.
76-4E	14	65G/2, 162742	Watterson Formation	Laminated micritic limestone and quartzose siltstone cut by quartz veins. Pyrite disseminations in micritic limestone to 0.025 mm; fractures in quartz veins filled with hematite and disseminated pyrite.
76-9A	15	65/G2, 169727	Watterson Formation	Thinly laminated siltstone and slate with iron sulphide and oxide alteration.
76-9B	15	65/G2, 169727	Watterson Formation	Calcareous siltstone with anastomosing pressure solution cleavage defined by hematite foliae; local disseminated pyrite (to 0.3 mm) and chalcopyrite. Microfractures in pyrite filled with hematite.
87-11	16	65G/2, 152703	Archean	Quartz vein cutting Archean granitic rocks; clusters of pyrite and chalcopyrite to 4 mm. Hematite alteration in fractures.
83-13	17	65G/2, 168693	Nueltin	Sulphide stain in satellite dyke cutting quartz arenite.
80-2	18	65G/2, 206685	Ameto Formation	Sulphide stained slate
80-3A	19	65G/2, 209684	Ameto Formation	Slate with cm-scale pyrite concretions distributed along bedding but elongate along cleavage.
80-3B	19	65G/2, 209684	Ameto Formation	Cryptalgal laminated microsparite with 2 mm pyrite disseminations (diagenetic ?) elongate along cleavage .
80-5A	20	65G/2, 213681	Ameto Formation	Laminated arkose, siltstone and slate in Bouma-like cycles with cm-dm-scale pyrite concretions (Fig. 10 A) and mm-scale disseminated pyrite.

TABLE II-1-C

SAMPLE	LOCALE	NTS/ UTM	UNIT	DESCRIPTION
80-5C	20	65G/2, 213681	Ameto Formation	Laminated arkose, siltstone and slate in Bouma-like cycles. Pyrite grains to 1 mm distributed along bedding engulfing detrital grains(diagenetic, Fig. 10 C); elongate along cleavage. Pyrite concretions to 1 cm distributed along arkosic layers but elongate along pressure solution cleavage; with quartz/chlorite fringes (Fig. 10 B). Hematite along cleavage foliae and as fracture fills.
80-5D	20	65G/2, 213681	Ameto Formation	Laminated arkose, siltstone, slate with pyrite concretions to 10 cm distributed along bedding. Local pyrrohtite disseminated in pyrite. Pyrite disseminations to 3mm, elongate along cleavage. Hematite in fractures and along pressure solution cleavage foliae.
80-5E	20	65G/2, 213681	Ameto Formation	Slate with pyrite concretions to 10 cm, distributed along bedding.
80-12	21	65G/2, 221680	Ameto Formation	Slate with pyrite concretions to 1 cm.
80-20B	22	65G/2, 216704	Ameto Formation	Arkose-slate Bouma-like cycles with pyrite concretions to 4 cm distributed along bedding.
94-8A	23	65B/15, 221611	Whiterock Member	Quartz arenite with disseminated pyrite to 1 cm cutting across polygonized quartz boundaries, internal fractures filled with hematite (Fig. 8 D).
94-8B	23	65B/15, 221611	Whiterock Member	Quartz arenite with disseminated pyrite to 8 mm along joints in boxwork structure. Crude layering along fracture defined by pyrite elongation and variation in pyrite concentration. Local pyrite disseminations in host to 4 mm.
91-13	24	65G/1, 288635	Whiterock Member	Quartz arenite with hematitic stain along joint surface.
98-18B	25	65G/1, 285654	Padlei Formation	Siltstone-shale rhythmites with hematitic stain along fractures.

TABLE II-1-D

SAMPLE	LOCALE	NTS/ UTM	UNIT	DESCRIPTION
S-4-C	26	65G/1, 274658	Hawk Hill Member	White laminar chert with crude bedding-parallel layering defined by variation in quartz crystal size, by wavy zones of hematite and chlorite alteration, and by local stylolitic surfaces.
S-10	26	65G/1, 274658	Hawk Hill Member	Breccia of white chert fragments in maroon chert/specular hematite cement.
S-11	26	65G/1, 274658	Hawk Hill Member	Breccia of white chert fragments in maroon chert/specular hematite cement.
88-13	27	65G/1, 272684	Maguse Member	Granulestone/arkose/shale interbeds with hematite (both detrital and from alteration of framework grains) and leucoxene disseminated in matrix.
88-4B	28	65G/2, 261676	Hawk Hill Member	Breccia of white chert fragments in maroon chert cement; void-filling specular hematite.
99-13B	29	65G/2, 247698	Maguse Member	Quartz arenite with hematitic stain along joint surface.
63-9A	30	65G/2, 246763	Archean	Arkose with disseminated pyrite.
63-9B	30	65G/2, 246763	Archean	Slate with sulphide stain adjacent quartz vein.
60-3	31	65G/2, 228778	Whiterock Member	Quartz arenite with hematitic stain along joint surface.
66-4B	32	65G/2, 226792	Whiterock Member	Quartz arenite with hematitic stain along joint surface.
66-10B	33	65G/2, 231789	Padlei Formation	Granule-pebble conglomerate with disseminated hematite, both detrital and from in situ alteration of framework grains.
68-6	34	65G/2, 238797	Whiterock Member	Quartz arenite with hematitic stain along joint surface.
73-6	35	65G/2, 223799	Whiterock Member	Quartz arenite with hematitic stain along bedding and joint surfaces.
73-7B	36	65G/2, 226801	Whiterock Member	Breccia of quartz arenite fragments in chlorite/specular hematite cement (Fig. 8 C).
71-5A	37	65G/2, 254819	Whiterock Member	Quartz arenite with hematitic stain along joint surfaces.
67-2B	38	65G/2, 243827	Ameto Formation	Slate with hematitic alteration along bedding, cleavage and fractures

TABLE II-1-E

SAMPLE	LOCALE	NTS/ UTM	UNIT	DESCRIPTION
72-7	39	65G/2, 246828	Ameto Formation	Slate with hematitic alteration along bedding, cleavage and fractures.
67-11	40	65G/2, 257835	Whiterock Member	Quartz arenite with hematitic stain along joint surfaces; hematite in mm-scale shear zones.
77-18	41	65G/2, 267853	Padlei Formation	Granule-pebble conglomerate; detrital hematite from magnetite-chert BIF clasts, detrital hematite, disseminated hematite from intrastratal solution.
78-11C	42	65G/2, 250860	Whiterock Member	Quartz arenite with hematitic stain along joint surface.
70-7	43	65G/2, 242884	Tavani Formation	Sub-arkose with lenses of cryptalgal laminate; pyrite-calcite-hematite in fractures.
79-1	44	65G/2, 254889	Archean	Arkosic siltstone with .05 mm pyrite (detrital ?) disseminated along bedding, and 1mm euhedral pyrite (with metamorphic quartz and chlorite rims).

TABLE II-2-A

METHOD		FADCP	DCP	DCP	DCP	DCP	DCP	DCP
LIMIT		1 PPB	100 ppm	100 ppm	10 ppm	100 ppm	10 ppm	2 ppm
ELEMENT		Au	Na	Mg	P	Ca	Ti	Cr
SAMPLE	LOCALE							
100-11A	1	>10,000 33,100* 7,980*	8400	4400	360	700	1400	32
100-11B	2	64	1000	31000	520	1300	2300	44
106-3	3	<1	300	200	80	200	80	10
97-11	4	23	400	800	30	400	170	26
96-2	5	230	900	23000	100	1300	400	14
97-1	6	<1	300	200	20	200	120	10
97-2	7	13	300	400	40	200	140	10
102-7	8	57	100	500	30	300	120	10
97-5A	9	<1	79000	1200	120	500	2800	36
97-5B	9	6	55000	7600	520	1800	2300	70
101-13	10	15	15000	3200	120	9400	2200	14
101-16	11	<1	49000	3300	730	1600	1500	8

* Fire assay by Terramin Research Laboratories Ltd.; S.Safton p. comm. 1990.

TABLE II-2-B

METHOD		FADCP	DCP	DCP	DCP	DCP	DCP	DCP
LIMIT		1 PPB	100 ppm	100 ppm	10 ppm	100 ppm	10 ppm	2 ppm
ELEMENT		Au	Na	Mg	P	Ca	Ti	Cr
SAMPLE	LOCALE							
101-33	12	23	100	1000	20	500	50	16
84-21	13	<1	900	1900	60	300	160	16
76-4E	14	<1	7100	25000	440	700	4800	110
76-9A	15	<1	900	56000	330	500	3900	90
76-9B	15	<1	2100	58000	1100	1500	22000	20
87-11	16	130	1300	1000	80	400	170	12
83-13	17	<1	37000	3800	110	1400	760	6
80-2	18	<1	900	44000	500	21000	3400	76
80-3A	19	4	900	52000	590	22000	3600	74
80-3B	19	<1	700	120000	170	54000	360	<2
80-5A	20	<1	800	48000	1000	23000	2200	50

TABLE II-2-C

METHOD		FADCP	DCP	DCP	DCP	DCP	DCP	DCP
LIMIT		1 PPB	100 ppm	100 ppm	10 ppm	100 ppm	10 ppm	2 ppm
ELEMENT		Au	Na	Mg	P	Ca	Ti	Cr
SAMPLE	LOCALE							
80-5C	20	<1	900	54000	670	36000	2300	48
80-5D	20	<1	1000	68000	480	58000	1800	34
80-5E	20	2	1000	56000	540	41000	2600	58
80-12	21	<1	900	45000	650	30000	2100	42
80-20B	22	<1	900	55000	410	38000	2800	62
94-8A	23	56	200	200	30	300	50	22
94-8B	23	80	200	300	<10	300	50	28
91-13	24	<1	<100	100	30	<100	40	4
98-18B	25	<1	29000	27000	650	4800	3100	110

TABLE II-2-D

	METHOD	FADCP	DCP	DCP	DCP	DCP	DCP	DCP
	LIMIT	1 PPB	100 ppm	100 ppm	10 ppm	100 ppm	10 ppm	2 ppm
ELEMENT		Au	Na	Mg	P	Ca	Ti	Cr
SAMPLE								
S-4-C	26	3	300	700	230	300	330	20
S-10	26	<1	300	1000	920	1800	460	20
S-11	26	<1	700	3400	9200	15000	570	34
88-13	27	<1	1000	9400	170	300	2300	38
88-4B	28	<1	200	420	2000	3500	110	20
99-13B	29	<1	200	1000	40	200	160	10
63-9A	30	<1	31000	20000	430	11000	1100	220
63-9B	30	<1	2800	8100	40	2000	190	32
60-3	31	<1	100	500	20	100	100	12
66-4B	32	<1	200	500	20	200	90	18
66-10B	33	2	1200	23000	220	700	5200	140
68-6	34	<1	<100	400	40	100	80	40
73-6	35	7	300	300	30	200	110	4
73-7B	36	460	500	300	70	300	220	12
71-5A	37	3	400	900	30	300	90	16
67-2B	38	3	1100	29000	540	800	3500	78

TABLE II-2-E

METHOD		FADCP	DCP	DCP	DCP	DCP	DCP	DCP
LIMIT		1 PPB	100 ppm	100 ppm	10 ppm	100 ppm	10 ppm	2 ppm
ELEMENT		Au	Na	Mg	P	Ca	Ti	Cr
SAMPLE	LOCALE							
72-7	39	<1	1200	29000	540	1000	6800	110
67-11	40	3	200	600	20	200	150	50
77-18	41	<1	800	14000	270	300	2100	100
78-11C	42	2	200	1400	40	300	320	16
70-7	43	<1	45000	20000	520	11000	2900	170
79-1	44	<1	31000	29000	590	6500	4200	200

TABLE II-3-A

METHOD		DCP	DCP	DCP	DCP	DCP	DCP	FAA	ICPMS
LIMIT		2 ppm	100 ppm	1.0 ppm	1.0 ppm	0.5 ppm	0.5 ppm	0.1 ppm	1.0 ppm
	ELEMENT	Mn	Fe	Co	Ni	Cu	Zn	As	Zr
SAMPLE	LOCALE								
100-11A	1	100	150,000	160	260	4.5	18.0	18.0	79
100-11B	2	1300	43000	150	130	3.5	5.5	25.0	30
106-3	3	10	24,000	99	19	3.0	6.5	2.1	13
97-11	4	30	5,900	5	4	4.5	7.5	42.0	18
96-2	5	790	47000	80	19	10.0	7.0	5.2	20
97-1	6	12	1100	5	12	2.0	2.5	0.4	9
97-2	7	72	3000	6	12	2.0	5.0	3.4	14
102-7	8	6	41,000	120	11	3.0	5.0	19.0	15
97-5A	9	12	22000	42	15	5.0	10.0	7.6	216
97-5B	9	34	74000	44	20	4.4	9.5	2.5	215
101-13	10	84	150000	130	56	24.0	71.0	45.0	130
101-16	11	42	18000	2	7	9.5	7.5	0.8	180

TABLE II-3-B

METHOD		DCP	DCP	DCP	DCP	DCP	DCP	FAA	ICPMS
LIMIT		2 ppm	100 ppm	1.0 ppm	1.0 ppm	0.5 ppm	0.5 ppm	0.1 ppm	1.0 ppm
	ELEMENT	Mn	Fe	Co	NI	Cu	Zn	As	Zr
SAMPLE	LOCALE								
101-33	12	160	17000	1	4	14.0	11.0	12.0	<1
84-21	13	6	11000	1	5	4.0	4.5	0.6	42
76-4E	14	34	20000	15	11	14.0	17	2.3	156
76-9A	15	150	17000	8	8	5.0	32.0	1.5	119
76-9B	15	140	29000	36	5	7.0	36.0	1.9	289
87-11	16	420	43000	11	6	1300	6.5	0.4	8
83-13	17	40	7000	5	8	41.0	6.0	0.7	144
80-2	18	810	47000	29	42	23.0	25.0	0.3	125
80-3A	19	810	45000	19	27	15.0	37.0	0.3	116
80-3B	19	3000	38000	9	6	5.0	11.0	0.5	28
80-5A	20	500	29000	14	23	11.0	41.0	3.6	124

TABLE II-3-C

METHOD		DCP	DCP	DCP	DCP	DCP	DCP	FAA	ICPMS
LIMIT		2 ppm	100 ppm	1.0 ppm	1.0 ppm	0.5 ppm	0.5 ppm	0.1 ppm	1.0 ppm
	ELEMENT	Mn	Fe	Co	Ni	Cu	Zn	As	Zr
SAMPLE	LOCALE								
80-5C	20	740	36000	13	39	11.0	62.0	3.0	104
80-5D	20	1200	40000	19	37	8.5	21.0	4.2	91
80-5E	20	770	21000	10	19	4.5	18.0	0.6	110
80-12	21	910	20000	9	9	9.0	21	0.3	66
80-20B	22	820	33000	18	20	10.0	20.0	6.8	98
94-8A	23	6	12000	4	5	4.5	5.0	0.6	2
94-8B	23	4	22000	9	5	5.0	3.5	3.3	308
91-13	24	10	31000	<1	<1	1.5	3.5	0.7	14
98-18B	25	420	43000	24	64	31.0	92.0	1.6	104

TABLE II-3-D

METHOD		DCP	DCP	DCP	DCP	DCP	DCP	FAA	ICPMS
LIMIT		2 ppm	100 ppm	1.0 ppm	1.0 ppm	0.5 ppm	0.5 ppm	0.1 ppm	1.0 ppm
	ELEMENT	Mn	Fe	Co	Ni	Cu	Zn	As	Zr
SAMPLE	LOCALE								
S-4-C	26	26	19000	1	7	4.5	4.0	1.4	14
S-10	26	68	33000	3	7	2.5	3.5	0.7	1
S-11	26	180	56000	8	36	4.0	6.0	3.6	11
88-13	27	56	26000	11	29	1.5	11.0	0.4	176
88-4B	28	52	20000	2	2	9.0	4.0	3.2	2
99-13B	29	4	2800	1	3	4.0	3.0	0.2	23
63-9A	30	620	37000	12	130	23.0	62.0	52.0	86
63-9B	30	160	12000	4	35	7.0	30.0	19.0	9
60-3	31	4	1100	<1	3	2.0	2.0	0.3	16
66-4B	32	10	1200	1	11	1.0	2.5	1.0	15
66-10B	33	250	77000	31	95	6.5	41.0	1.0	94
68-6	34	6	1400	1	4	1.0	2.5	0.3	13
73-6	35	12	800	4	8	3.5	2.5	0.4	4
73-7B	36	34	25000	4	11	6.5	4.0	5.2	28
71-5A	37	10	900	1	3	1.5	3.0	0.5	17
67-2B	38	170	66000	21	75	67.0	50.0	2.4	134

TABLE II-3-E

METHOD		DCP	DCP	DCP	DCP	DCP	DCP	FAA	ICPMS
LIMIT		2 ppm	100 ppm	1.0 ppm	1.0 ppm	0.5 ppm	0.5 ppm	0.1 ppm	1.0 ppm
	ELEMENT	Mn	Fe	Co	Ni	Cu	Zn	As	Zr
SAMPLE	LOCALE								
72-7	39	220	90000	33	93	7.5	58.0	3.2	136
67-11	40	24	16000	2	6	3.0	2.5	0.7	12
77-18	41	130	55000	18	65	5.5	24.0	1.2	103
78-11C	42	14	11000	5	3	2.0	3.0	6.2	17
70-7	43	530	29000	15	74	15.0	15.0	3.2	122
79-1	44	680	58000	30	170	35.0	57.0	3.8	79

TABLE II-4-A

METHOD		DCP	DCP	DCP	ICPMS	FAA	ICPMS
LIMIT		1.0 ppm	0.5 ppm	1.0 ppm	1.0 ppm	0.1 ppm	1.0 ppm
	ELEMENT	Mo	Ag	Cd	Sn	Sb	Ba
SAMPLE	LOCALE						
100-11A	1	<1	<0.5	<1	1	2.0	15
100-11B	2	6	<0.5	<1	1	1.0	2200
106-3	3	<1	<0.5	<1	<1	0.2	90
97-11	4	<1	<0.5	<1	<1	0.4	51
96-2	5	5	<0.5	1	<1	0.6	57
97-1	6	2	<0.5	<1	<1	0.3	1[illegible]
97-2	7	3	<0.5	<1	<1	0.4	18
102-7	8	<1	<0.5	<1	<1	0.2	24
97-5A	9	3	1.0	<1	1	0.4	58
97-5B	9	3	0.5	<1	<1	0.4	90
101-13	10	10	<0.5	<1	2	0.6	25
101-16	11	5	<0.5	<1	<1	0.3	3300

TABLE II-4-B

METHOD		DCP	DCP	DCP	ICPMS	FAA	ICPMS
LIMIT		1.0 ppm	0.5 ppm	1.0 ppm	1.0 ppm	0.1 ppm	1.0 ppm
	ELEMENT	Mo	Ag	Cd	Sn	Sb	Ba
SAMPLE	LOCALE						
101-33	12	<1	<0.5	<1	<1	0.2	15
84-21	13	<1	<0.5	<1	<1	0.2	4
76-4E	14	4	<0.5	<1	6	0.3	3500
76-9A	15	3	<0.5	<1	2	0.4	437
76-9B	15	7	<0.5	1	2	0.5	767
87-11	16	<1	<0.5	<1	<1	<0.1	58
83-13	17	3	<0.5	1	2	0.2	61
80-2	18	2	<0.5	<1	2	0.2	290
80-3A	19	2	<0.5	1	1	0.3	266
80-3B	19	<1	<0.5	<1	<1	<0.1	49
80-5A	20	1	<0.5	1	1	0.6	258

TABLE II-4-C

	METHOD	DCP	DCP	DCP	ICPMS	FAA	ICPMS
	LIMIT	1.0 ppm	0.5 ppm	1.0 ppm	1.0 ppm	0.1 ppm	1.0 ppm
	ELEMENT	Mo	Ag	Cd	Sn	Sb	Ba
SAMPLE	LOCALE						
80-5C	20	1	<0.5	<1	<1	0.4	228
80-5D	20	<1	<0.5	<1	1	0.3	190
80-5E	20	1	<0.5	<1	1	0.3	276
80-12	21	1	<0.5	<1	<1	0.3	303
80-20B	22	1	<0.5	<1	1	0.3	242
94-8A	23	<1	<0.5	<1	<1	1.3	17
94-8B	23	<1	<0.5	<1	<1	0.6	11
91-13	24	<1	<0.5	<1	<1	0.2	8
98-18B	25	2	<0.5	<1	1	0.5	700

TABLE II-4-D

METHOD		DCP	DCP	DCP	ICPMS	FAA	ICPMS
LIMIT		1.0 ppm	0.5 ppm	1.0 ppm	1.0 ppm	0.1 ppm	1.0 ppm
	ELEMENT	Mo	Ag	Cd	Sn	Sb	Ba
SAMPLE	LOCALE						
S-4C	26	3	<0.5	<1	<1	0.8	42
S-10	26	3	<0.5	<1	<1	0.8	48
S-11	26	5	<0.5	<1	<1	0.5	125
88-13	27	2	<0.5	<1	<1	0.4	710
88-4B	28	<1	<0.5	<1	<1	0.7	154
99-13B	29	<1	<0.5	<1	<1	0.3	66
63-9A	30	5	1.0	<1	<1	0.4	700
63-9B	30	2	0.5	<1	<1	0.1	69
60-3	31	<1	<0.5	<1	<1	<0.1	32
66-4B	32	<1	0.5	<1	<1	<0.1	81
66-10B	33	7	2.0	<1	1	0.4	591
68-6	34	<1	<0.5	<1	<1	<0.1	17
73-6	35	3	<0.5	1	<1	0.8	20
73-7B	36	4	<0.5	<1	<1	0.8	24
71-5A	37	<1	<0.5	<1	<1	<0.1	34
67-2B	38	6	1.0	<1	2	0.2	385

TABLE II-4-E

METHOD		DCP	DCP	DCP	ICPMS	FAA	ICPMS
LIMIT		1.0 ppm	0.5 ppm	1.0 ppm	1.0 ppm	0.1 ppm	1.0 ppm
	ELEMENT	Mo	Ag	Cd	Sn	Sb	Ba
SAMPLE	LOCALE						
72-7	39	8	2.0	<1	2	0.1	211
67-11	40	1	<0.5	<1	<1	0.4	20
77-18	41	2	<0.5	<1	<1	1.0	424
78-11C	42	<1	<0.5	<1	<1	0.4	434
70-7	43	6	1.5	<1	<1	<0.1	206
79-1	44	10	<0.5	2	<1	0.7	397

TABLE II-5-A

METHOD		ICPMS	DCP	FAA	ICPMS	ICPMS
LIMIT		1.0 ppm	1.0 ppm	0.1 ppm	0.1 ppm	0.1 ppm
ELEMENT		W	Pb	Bi	Th	U
SAMPLE	LOCALE					
100-11A	1	5	<2	0.9	1.4	1.4
100-11B	2	8	<2	0.6	11.2	3.2
106-3	3	<1	<2	0.1	1.9	0.4
97-11	4	<1	<2	0.3	1.2	0.6
96-2	5	2	<2	0.2	2.3	0.6
97-1	6	<1	<2	<0.1	0.6	<0.1
97-2	7	<1	0.4	<0.1	1.0	0.4
102-7	8	<1	<2	1.1	0.8	0.3
97-5A	9	4	<2	0.9	1.4	1.4
97-5B	9	<1	<2	0.8	10.7	2.4
101-13	10	1	6	0.9	2.1	0.7
101-16	11	4	4	0.2	41.4	6.4

TABLE II-5-B

METHOD		ICPMS	DCP	FAA	ICPMS	ICPMS
LIMIT		1.0 ppm	1.0 ppm	0.1 ppm	0.1 ppm	0.1 ppm
ELEMENT		W	Pb	Bi	Th	U
SAMPLE	LOCALE					
101-33	12	<1	<2	0.2	0.1	0.2
84-21	13	<1	<2	0.2	3.3	0.9
76-4E	14	2	<2	0.3	25.3	4.2
76-9A	15	<1	<2	0.2	7.7	5.5
76-9B	15	1	<2	0.3	4.6	2.5
87-11	16	<1	100	<0.1	0.6	0.5
83-13	17	<1	<2	0.6	44.0	7.9
80-2	18	<1	<2	0.2	6.6	1.4
80-3A	19	<1	26	0.2	6.2	1.3
80-3B	19	<1	<2	<0.1	1.1	0.4
80-5A	20	<1	<2	0.1	5.7	1.4

TABLE II-5-C

METHOD		ICPMS	DCP	FAA	ICPMS	ICPMS
LIMIT		1.0 ppm	1.0 ppm	0.1 ppm	0.1 ppm	0.1 ppm
ELEMENT		W	Pb	Bi	Th	U
SAMPLE	LOCALE					
80-5C	20	<1	<2	<0.1	4.7	1.4
80-5D	20	<1	34	<0.1	4.7	1.1
80-5E	20	<1	<2	<0.1	5.8	1.5
80-12	21	<1	320	<0.1	4.6	1.4
80-20B	22	<1	<2	0.3	5.4	1.3
94-8A	23	<1	<2	0.4	0.3	0.2
94-8B	23	<1	<2	0.4	0.2	293
91-13	24	<1	<2	<0.1	1.0	0.8
98-18B	25	1	<2	<0.1	8.0	2.1

TABLE II-5-D

METHOD		ICPMS	DCP	FAA	ICPMS	ICPMS
LIMIT		1.0 ppm	1.0 ppm	0.1 ppm	0.1 ppm	0.1 ppm
ELEMENT		W	Pb	Bi	Th	U
SAMPLE	LOCALE					
S-4C	26	6	<2	0.2	0.9	1.7
S-10	26	7	<2	0.3	0.3	0.4
S-11	26	19	<2	0.3	3.0	1.3
88-13	27	<1	260	0.2	8.0	2.6
88-4B	28	17	<2	0.1	0.4	1.4
99-13B	29	2	68	<0.1	1.0	0.8
63-9A	30	<1	6	1.0	5.0	1.5
63-9B	30	<1	10	0.3	0.8	0.3
60-3	31	<1	4	<0.1	1.2	0.5
66-4B	32	1	4	<0.1	0.9	0.4
66-10B	33	4	<2	<0.1	4.2	2.4
68-6	34	3	<2	<0.1	0.9	0.5
73-6	35	<1	<2	<0.1	0.7	0.2
73-7B	36	1	<2	0.3	1.2	0.4
71-5A	37	2	2	<0.1	1.0	1.6
67-2B	38	1	6	0.3	16.1	3.0

TABLE II-5-E

METHOD		ICPMS	DCP	FAA	ICPMS	ICPMS
LIMIT		1.0 ppm	1.0 ppm	0.1 ppm	0.1 ppm	0.1 ppm
ELEMENT		W	Pb	Bi	Th	U
SAMPLE	LOCALE					
72-7	39	2	<2	0.6	5.2	1.4
67-11	40	6	4	<0.1	0.9	0.4
77-18	41	<1	<2	0.2	7.3	1.9
78-11C	42	<1	<2	0.1	0.8	0.5
70-7	43	3	<2	0.1	11.6	2.2
79-1	44	<1	<2	0.2	5.9	1.6

TABLE III SUMMARY OF GOLD VALUES

(SEE TABLE II FOR FULL ANALYTICAL RESULTS AND PETROGRAPHIC DESCRIPTIONS; FIGURE 7 FOR LOCATIONS)

UNIT	GOLD (ppb)	COMMENT
TAVANI FORMATION	**6**; sample 97-5B locality 9	brecciated sub-arkose with lenses of cryptalgal laminate; pyrite-hematite calcite
WATTERSON FORMATION	**>10,000; 33,100 7,980** sample 100-11A, locality 1; **64** sample 100-11B, locality 2	pyrite-quartz stockwork, calcareous arkose (locality 1) disseminated diagenetic (?) pyrite calcareous siltstone, locality 2
AMETO FORMATION	**4**, sample 80-3A, locality 19;**2**, sample 80-5E, locality 20	pre-strain (diagenetic?) pyrite concretions in laminated arkose/siltstone/slate
HAWK HILL MEMBER, KINGA FORMATION	**3**, sample S-4-C, locality 26	white laminar silcrete with wavy zones of hematite/chlorite alteration
WHITEROCK MEMBER, KINGA FORMATION	**460**, sample 73-7B, locality 36	quartz arenite breccia with specular hematite cement
	23, sample 97-11, locality 4; **230**, sample 96-2, locality 5; **13**, sample 97-2, locality 7; **57**, sample 102-7, locality 8; **23**, sample 101-33, locality 12; **56**, sample 94-8A, **80** sample 94-8B, locality 23	quartz arenite with pyrite-quartz along fractures and pyrite disseminations adjacent to fractures
	7, sample 73-6, locality 35; **3**, sample 71-5A, locality 37; **3**, sample 67-11, locality 40; **2**, sample 78-11C, locality 42.	quartz arenite with local hematitic stain along fractures
PADLEI FORMATION	2, sample 66-10B, locality 33	conglomerate with BIF clasts; detrital and diagenetic hematite

Proterozoic quartz vein cutting Archean granite	130, sample 87-11, locality 16.	pyrite and chalcopyrite clusters
ARCHEAN MAFIC TUFF	15, sample 101-13, locality 10	pyrite concentrations along layering